

Ref.: " *Evaluation of Lacustrine Groundwater Discharge, Hydrologic Partitioning, and Nutrient Budgets in a Proglacial Lake in Qinghai-Tibet Plateau: Using ^{222}Rn and Stable Isotopes*" (Dr. Xin Luo)

Editor

I received comments from two reviewers, both suggested "minor revision". The reviewers are generally positive to the manuscript, but pinpoint some revisions needed to be done before its acceptance. After receiving the comments, I carefully read the manuscript again, and concur with the reviewers. Please reply to the comments/questions in detail and revise your manuscript accordingly.

- We appreciate the overall positive comments for this study. In the revised MS, we have addressed all the comments raised by the two reviewers in details as shown below.
- We have also checked the MS carefully for typos, missing authors, and their affiliations, terminology, updates of data in tables, and updates of variables in equations.

Reviewer #1

General comments: This paper is focusing on the evaluation of LGD and its related nutrient budgets and hydrologic partitioning in proglacial lake of QTP. The work is great and the paper is overall well organized. Anyway, I have the following comments for the authors to consider.

Reply to General comments:

- We appreciate the overall positive comments for this study.

Specific comments

1. Authors should address more about why it's important to study proglacial lake, especially the ones in QTP, in the introduction part.

- Well taken. We have added more description of the proglacial lakes, and lake dynamics in QTP under the influence of climate change and global warming. Some latest lake studies in the QTP were also reviewed (lines 81-104).

2. The primary productivity is calculated based on the dissolved inorganic nutrient budgets. Authors should be careful to do so. Did the authors consider the transformation between dissolved inorganic and particulate inorganic forms? Redfield ratio usually works in oceanic aquatic system. In lakes, the ratio is fairly variable.

- Good question, indeed, we noticed that the DIN and DIP relation cannot be used to quantify the primary production in the fresh lacustrine systems due to the high variability of Redfield ratios and the possibility of transformation between DIN/DIP. Based on the measurement results, DIN: DIP ratios in the lake water and groundwater are all much large than 16:1, indicating the phosphate limited conditions.
- As indicated by previous studies of glacial melting water bodies in the QTP, Arctic and Antarctic, the dominant form of dissolve phosphate is DIP, while the DOP contributes less than 10 % of the dissolved phosphate (Hawkings et al. 2016, Hodson 2007, Hodson et al. 2005, Liu et al. 2011, Mitamura et al. 2003). In the freshwater system, particular phosphate is highly bounded. Therefore, it is reasonable to assume that primary production in the lake

water is limited by DIP, and to assign glacial melting water as phosphate limited condition in this study.

- The primary producers in the lake system consume the nutrient production under variant N: P ratios as indicated by previous studies (Downing and McCauley 1992). To avoid the ambiguous statements and conclusions, we discussed this term as the biological uptake/transformation of nutrients, and removed the ambiguous statements on primary production throughout the MS (lines 756-800).

3. Radon in air is important term to do balance calculation. Was the Rn in air measured? I did not see the information or data about this term in the manuscript or the SI.

- Yes, we placed RAD7 for air radon-222 measurement at the lake shore for about 4 hours, and the mean activity of the lake area is $1.51 \pm 0.97 \text{ Bq m}^{-3}$. We added the ambient air radon-222 activities in Table 1 and some descriptions in the methodology part (lines 268-271).

4. Line 53-60, these two sentences are both started with the locations. Please revise them.

- Well taken, these sentences were revised as suggested (lines 76-77).

5. Line 208, how often were the Ra-226 samples collected? Or just one sample, and you assume Ra-226 is constant? 6. Line 279, how long is t ? 7. Line 327, figure 5 is not attached.

- Due to the bad weather condition and large sampling volume, we could only obtain one ^{226}Ra sample. However, radium in the lacustrine system is significantly lower compared to ^{222}Rn , therefore, the decay input of ^{222}Rn from ^{226}Ra is minimal and negligible. Thus, the spatial heterogeneity of radon-222 will mount minimal effects on the final ^{222}Rn mass balance models.
- The time step is set to be 5 min, in consistent with the ^{222}Rn record interval. More statements were added in the revised MS (lines 365-366).
- Figure 5 was attached in the revised MS.

Technical corrections

1. Line 144, 0.7 or 7?

- Well taken, this is 0.7 m s^{-1} , and change was made in the revision MS (line 205).

2. Line 195, the unit should be L min^{-1} .

- Well taken, unit was change to L min^{-1} (line 256).

3. Line 230, change “recently” to “recent”.

- Well taken, change was made (line 302).

4. Line 280, should be Equation (2).

- Well taken, change was made (line 367).

5. Line 383, two 180?

- Typo and change was made (line 477).

Reviewer #2

General comments: This is an interesting and generally well-written paper that makes a good contribution to understanding the groundwater surface water interactions and estimating the lacustrine groundwater discharge in mountainous proglacial lakes in the QTP. The abstract is correctly informative with some remarks (see below). The introduction and the site description take into account previous papers in exhaustive way. The methodological approach for data analysis is modern without particular novelties. High-resolution ^{222}Rn activities, water level, both in water temperature and, wind speed together with stable isotopic data are quite impressive. Many studies have done to explain the high single digits in the whole paper.

- We appreciated the overall positive comments.

4. Discussion

Do the adjoining lacustrine aquifers receive ('recharge') to sustain the inferred rate of groundwater discharge? And is the inferred width of the zone of lacustrine groundwater discharge compatible with the physics of the groundwater flow system and hydrological cycle?

- The regional precipitation recorded by the Jiuzhi station is to be around 90 mm d^{-1} during Aug, 2015. When deploying an empirical infiltration coefficient of 0.2 for the lake basin, the aquifer recharge rates are yielded up to 18 mm d^{-1} , which is sufficient to maintain the water balance within the lacustrine aquifers. Moreover, as indicated by previous studies in an interior lake of the QTP, Nam Co, a lake located at the area with relatively high evaporation and lower precipitation, its LGD is estimated to be $5\text{-}8 \text{ mm d}^{-1}$ and is comparable to the results of this study. This also indirectly implicate that the LGD in this study is tenable and can be balanced by the recharge of the lacustrine aquifers, as Ximen Co basin is influenced by rather larger precipitation and lower evaporation compared to Nam Co.
- The inferred width of the zones of lacustrine groundwater discharge is also regarded as the seepage face. Previous studies have indicated that the groundwater seepage areas are mostly located along the transect within 10-20 m across the lakeshore (Luo et al. 2016, Luo et al. 2017, Rosenberry et al. 2015, Schafran and Driscoll 1993). While the deep groundwater system is rather constrained by the Precambrian bedrocks (Einarsdottir et al. 2017), and the LGD occurrence is considered to be constrained within the seepage faces along the lakeshores, and within the bathymetry of epilimnion.

Did you consider the lag time between recharge and chemical changes in the lacustrine aquifers?

- The lag time between the recharge and the chemical changes in the lacustrine aquifers is not considered in this study for the following reasons: (1) For ^{222}Rn , the equilibrium state is assigned as ^{222}Rn will reach equilibrium states within short distance (sever centimeters) and elapsed time after the infiltration (Ku et al. 1992, Porcelli 2008). (2) Stable isotopes generally behave rather conservatively after entering the aquifer and there is negligible fractionation during the transport in the aquifer between the recharge and discharge. (3) The groundwater sampling locations were located at the immediate zones of the lake shore, and therefore, the dynamics the flow length and recharge lag time is minimal and negligible for the reactive

solutes of DIN and DIP, similar as suggested in many previous studies (Dimova and Burnett 2011, Dimova et al. 2013, Kluge et al. 2012, Luo et al. 2016).

Please consider the relationship between Fig 5 and Fig 6 to give a relevant illustration on chemical components and isotopic data.

- We are sorry that we forgot to attach Figure 5 in the previous version. This figure was used to give a relevant illustration on chemical components and isotopic data.

Fig. 6 The conceptual model of ^{222}Rn transient model looks well. But the associated illustration in the text is not convincing on the flow pathways for the ^{222}Rn sources. Clearly some components of the conceptual understanding are not supported by the data. The manuscript would also benefit greatly from a more thorough literature review, which in-turn will help establish the objectives of the work. My main concern with the paper is with the ^{222}Rn analysis that I don't think is well enough explained to be convincing. Doing a more thorough job on this will add material.

- If we understood properly, this comment has two points: reliability of some components and literature review. The reviewer did not specify which components that were not supported by the data. We guess they could be lake evaporation and riverine inflow. To take account this comment, we have reviewed more relevant literatures and added more discussion on lake evaporation and riverine inflow (lines 684 to 713).

Conclusions

This section just summarizes the main findings of the project. In the introduction you make some general statements about the need to understand processes in these impacted lacustrine aquifers in general. In this section explain in more detail how your project helps us to understand processes in these environments more broadly; the paper will have more impact if researchers from elsewhere in the world can see relevance to their studies and a paper in a major international journal such as HESS needs to have broad appeal

- To stress the research significance of this study, we have added more discussions to explain how the results of this study facilitate the understanding the environments more broadly (lines 857-863). We hope the updated MS can meet the board research interest of HESS.

References

- Dimova, N.T. and Burnett, W.C. (2011) Evaluation of groundwater discharge into small lakes based on the temporal distribution of radon-222. *Limnol. Oceanogr* 56(2), 486-494.
- Dimova, N.T., Burnett, W.C., Chanton, J.P. and Corbett, J.E. (2013) Application of radon-222 to investigate groundwater discharge into small shallow lakes. *Journal of Hydrology*.
- Downing, J.A. and McCauley, E. (1992) The nitrogen: phosphorus relationship in lakes. *Limnology and Oceanography* 37(5), 936-945.
- Einarsdottir, K., Wallin, M.B. and Sobek, S. (2017) High terrestrial carbon load via groundwater to a boreal lake dominated by surface water inflow. *Journal of Geophysical Research: Biogeosciences*, n/a-n/a.
- Hawkings, J., Wadham, J., Tranter, M., Telling, J., Bagshaw, E., Beaton, A., Simmons, S.L., Chandler, D., Tedstone, A. and Nienow, P. (2016) The Greenland Ice Sheet as a hot spot of phosphorus weathering

and export in the Arctic. *Global Biogeochemical Cycles*.

Hodson, A. (2007) Phosphorus in glacial meltwaters. *Glacier Science and Environmental Change*, 81-82.

Hodson, A., Mumford, P., Kohler, J. and Wynn, P.M. (2005) The High Arctic glacial ecosystem: new insights from nutrient budgets. *Biogeochemistry* 72(2), 233-256.

Kluge, T., von Rohden, C., Sonntag, P., Lorenz, S., Wieser, M., Aeschbach-Hertig, W. and Illmer, J. (2012) Localising and quantifying groundwater inflow into lakes using high-precision ^{222}Rn profiles. *Journal of Hydrology*.

Ku, T.-L., Luo, S., Leslie, B. and Hammond, D. (1992) Uranium-series disequilibrium: applications to earth, marine, and environmental sciences. 2. ed.

Liu, Y., Yao, T., Jiao, N., Tian, L., Hu, A., Yu, W. and Li, S. (2011) Microbial diversity in the snow, a moraine lake and a stream in Himalayan glacier. *Extremophiles* 15(3), 411-421.

Luo, X., Jiao, J.J., Wang, X.-s. and Liu, K. (2016) Temporal ^{222}Rn distributions to reveal groundwater discharge into desert lakes: implication of water balance in the Badain Jaran Desert, China. *Journal of Hydrology* 534, 87-103.

Luo, X., Jiao, J.J., Wang, X.-s., Liu, K., Lian, E. and Yang, S. (2017) Groundwater discharge and hydrologic partition of the lakes in desert environment: Insights from stable ^{18}O and radium isotopes. *Journal of Hydrology* 546, 189-203.

Mitamura, O., Seike, Y., Kondo, K., Goto, N., Anbutsu, K., Akatsuka, T., Kihira, M., Tsering, T.Q. and Nishimura, M. (2003) First investigation of ultraoligotrophic alpine Lake Puma Yumco in the pre-Himalayas, China. *Limnology* 4(3), 167-175.

Porcelli, D. (2008) Investigating groundwater processes using U- and Th-series nuclides. *Radioactivity in the Environment* 13, 105-153.

Rosenberry, D.O., Lewandowski, J., Meinikmann, K. and Nützmann, G. (2015) Groundwater - the disregarded component in lake water and nutrient budgets. Part 1: effects of groundwater on hydrology. *Hydrological Processes* 29(13), 2895-2921.

Schafran, G.C. and Driscoll, C.T. (1993) Flow path-composition relationships for groundwater entering an acidic lake. *Water Resources Research* 29(1), 145-154.

1 *Revised MS submitted to HESS*

Deleted: Confidential

2 **Evaluation of Lacustrine Groundwater Discharge, Hydrologic**
3 **Partitioning, and Nutrient Budgets in a Proglacial Lake in**
4 **Qinghai-Tibet Plateau: Using ²²²Rn and Stable Isotopes**

6 **Xin LUO^{1,2,3}, Xingxing Kuang⁴, Jiu Jimmy Jiao^{1,2,3*}, Sihai, Liang⁵, Rong Mao^{1,2}**
7 **⁴, Xiaolang Zhang^{1,2,4}, and Hailong Li⁴**

Deleted: X

Deleted: ³

Deleted: Liang⁴

Deleted: ³

Deleted: ³

Deleted: Li³

9 ¹Department of Earth Sciences, The University of Hong Kong, P. R. China

10 ²The University of Hong Kong, Shenzhen Research Institute (SRI), Shenzhen, P. R.
11 China

12 ³The University of Hong Kong-Zhejiang Institute of Research and Innovation
13 (HKU-ZIRI), Hangzhou, PR China

Formatted: Superscript

14 ⁴School of Environmental Science and Engineering, Southern University of Science
15 and Technology, 1088 Xueyuan Rd., Shenzhen, China,

Deleted: ³

16 ⁵School of Water Resources & Environment, China University of Geosciences, 29
17 Xueyuan Road, Beijing, China

Deleted: School of Environmental Science and Engineering, South University of Science and Technology of China (SUSTC), Shenzhen, China.

Deleted: ⁴School

21 Corresponding author: Jiu Jimmy Jiao (jjiao@hku.hk)

22 Department of Earth Sciences, The University of Hong Kong

23 Room 302, James Lee Science Building, Pokfulam Road, Hong Kong

24 Tel (852) 2857 8246; Fax (852) 2517 6912

25

39 | **Abstract**

Deleted: -

-

40 | Proglacial lakes are good natural laboratories to investigate groundwater and

41 | glacier dynamics under current climate condition and to explore [biogeochemical](#)

Deleted: primary productivity

42 | [cycling](#) under pristine lake status. This study conducted a series of investigations of

43 | ^{222}Rn , stable isotopes, nutrients and other hydrogeochemical parameters in Ximen Co

44 | Lake, a remote proglacial lake in the east of Qinghai-Tibet Plateau (QTP). A radon

45 | mass balance model was used to quantify the lacustrine groundwater discharge (LGD)

46 | of the lake, leading to an LGD estimate of $10.3 \pm 8.2 \text{ mm d}^{-1}$. Based on the three end

47 | member models of stable ^{18}O and Cl^- , the hydrologic partitioning of the lake is

48 | obtained, which shows that groundwater discharge only accounts for 7.0 % of the

49 | total water input. The groundwater derived DIN and DIP loadings constitute 42.9 %

50 | and 5.5 % of the total nutrient loading to the lakes, indicating the significance of LGD

51 | in delivering disproportionate DIN into the lake. [This study presents the first attempt](#)

Deleted: The primary productivity of the lake water is calculated to be $0.41 \text{ mmol C m}^{-2} \text{ d}^{-1}$.

52 | to evaluate the LGD and hydrologic partitioning in the glacial lake by coupling

Deleted: s

53 | radioactive and stable isotopic approaches and the findings advance the understanding

54 | of nutrient budgets [in the proglacial lakes of QTP](#). The study is also instructional in

Deleted: and primary productivity

55 | revealing the hydrogeochemical processes in proglacial lakes elsewhere.

56 | **Keywords:** Proglacial lake; ^{222}Rn ; lacustrine groundwater discharge; hydrologic

57 | partitioning; nutrient budgets

Deleted: ; primary productivity

67 **1. Introduction**

68 High altitude and latitude areas are intensively influenced by the melting of
69 glaciers due to climatic warming. Of particular importance are the proglacial areas,
70 such as proglacial lakes and moraines, because they are particularly affected by
71 climatic change induced glacier retreating and thawing of permafrost (Heckmann et
72 al., [2016](#); Barry, 2006; Slaymaker, 2011). The proglacial lakes are usually located close
73 to ice front of a glacier, ice cap or ice sheet, with the vicinity to the ice front
74 sometimes defined as the areas with subrecent moraines and formed by the last
75 significant glacier advances at the end of the Little Ice Age (Heckmann et al.,
76 [2016](#); Barry, 2006; Slaymaker, 2011; Harris et al., 2009). [These](#) lakes are located in the
77 transition zones from glacial to non-glacial conditions, [and can serve as](#) natural
78 laboratories to explore hydrological processes, biogeochemical cycles and
79 geomorphic dynamics under current climatic conditions (Dimova et al.,
80 2015; Heckmann et al., 2015).

81 [The Qinghai-Tibet Plateau \(QTP\), the third pole of the world, serves as the water](#)
82 [tower of most of the major rivers in Asian](#) (Qiu, 2008). [Unique landscapes such as endorheric](#)
83 [lakes, permafrost, glaciers, and headwater fluvial networks are developed due to the](#) [intensive](#)
84 [interaction between the atmosphere, hydrosphere, biosphere and cryosphere](#) (Lei et al.,
85 2017; Zhang et al., 2017a; Zhang et al., 2017b; Yao et al., 2013; Yao et al., 2012). [Distributed](#)

Deleted: 2015

Deleted: 2015

Deleted: Proglacial

Deleted: providing

Deleted: (Qiu 2008)

Deleted: coherent

92 mountainous glaciers and lakes are the most representative landscapes and are highly
93 sensitive to the climate changes. In the past decade, the lakes in the interior of the QTP show
94 overall expanding with respect to an overall increase of precipitation, accelerated glacier
95 melting and permafrost degradation (Zhang et al., 2013;Zhang et al., 2017b;Zhang et al.,
96 2017a;Heckmann et al., 2016;Yang et al., 2014). Some latest studies have made effects to
97 depict the hydrologic partitioning of the majority of the lakes in the QTP based on long term
98 observation of climatological parameters, and remote sensing approaches. However, so far a
99 quantitative evaluation of the water balance and hydrologic partitioning, especially the
100 groundwater component of the lakes in the QTP is limited due to the scarcity of observational
101 data. Therefore, there is a great need to conduct refined and systematical field observation to
102 provide groundtruth dataset and tenable models to depict the water balance and hydrologic
103 partitioning of the lakes, especially proglacial lakes in the QTP (Yang et al., 2014;Zhang et al.,
104 2017b).

Deleted: and deepening

Deleted: as far as now,

Deleted: refining and

Deleted: led

Deleted: ed

105 Mountainous proglacial lakes, formed by glacial erosion and filled by melting
106 glaciers, are widely distributed in the Qinghai-Tibet Plateau (QTP), especially along
107 the substantial glacier retreating areas of Himalaya Mountains (MT.), Qilian MT.,
108 Tienshan MT., etc. Characterized by higher elevations, small surface areas but
109 relatively large depths, mountainous proglacial lakes in QTP lack systematic
110 field-based hydrological studies due to their remote locations and difficulty in

Deleted:

117 | conducting field work (Yao et al., 2012;Farinotti et al., 2015;Bolch et al., 2012).

118 | There has been extensive recognition of the importance of groundwater discharge
119 | to various aquatic systems for decades (Dimova and Burnett, 2011;Valiela et al.,
120 | 1978;Johannes, 1980). Very recently, the topic of ‘lacustrine groundwater discharge
121 | (LGD)’, which is comprehensively defined as groundwater exfiltration from lake
122 | shore aquifers to lakes (Lewandowski et al., 2015;Rosenberry et al., 2015;Blume et al.,
123 | 2013;Lewandowski et al., 2013), has been introduced. LGD is analogous of in
124 | submarine groundwater discharge (SGD) in coastal environments. LGD [also](#) plays a
125 | vital role in lake hydrologic partitioning, which is defined as the separation of
126 | groundwater discharge/exfiltration, riverine inflow, riverine outflow infiltration,
127 | surface evaporation and precipitation for the hydrological cycle of the lake (Luo et al.,
128 | 2017;Good et al., 2015). LGD also serves as an importance component in delivering
129 | solutes to lakes since groundwater is usually concentrated in nutrients, CH₄, dissolved
130 | inorganic/organic carbon (DIC/DOC) and other geochemical components (Paytan et
131 | al., 2015;Lecher et al., 2015;Belanger et al., 1985;Dimova et al., 2015). Nutrients and
132 | carbon loading from groundwater greatly influences ratios of dissolved inorganic
133 | nitrogen (DIN) to dissolved inorganic phosphate (DIP) (referred as N: P ratios
134 | thereafter), ecosystem structure and the primary productivity of the lake aquatic
135 | system (Nakayama and Watanabe, 2008;Belanger et al., 1985;Hagerthey and Kerfoot,

136 1998).

137 The approaches to investigate LGD include, 1) direct seepage meters (Shaw and
138 Prepas, 1990;Lee, 1977), 2) geo-tracers such as radionuclides, stable ^2H and ^{18}O
139 isotopes (Gat, 1995;Kluge et al., 2007;Kraemer, 2005;Lazar et al., 2008), 3) heat and
140 temperature signatures (Liu et al., 2015;Sebok et al., 2013), 4) numerical modeling
141 (Winter, 1999;Smerdon et al., 2007;Zlotnik et al., 2009;Zlotnik et al., 2010) and 5)

142 remote sensing (Lewandowski et al., 2013;Wilson and Rocha, 2016;Anderson et al.,
143 2013). Recently, some researchers started to investigate groundwater dynamics in
144 peri- and proglacial areas, mostly based on the approaches of numerical modeling
145 (Lemieux et al., 2008b;Lemieux et al., 2008c;Andermann et al., 2012;Scheidegger
146 and Bense, 2014;Lemieux et al., 2008a). However, the quantification of groundwater
147 and surface water exchange in proglacial lakes is still challenging due to limited
148 hydrogeological data and extremely seasonal variability of aquifer permeability
149 (Dimova et al., 2015;Callegary et al., 2013;Xin et al., 2013).

150 ^{222}Rn , a naturally occurring inert gas nuclide highly concentrated in groundwater,
151 can be more applicable in fresh aquatic systems and has been widely used as a tracer
152 to quantify groundwater discharge in fresh water lakes (Luo et al., 2016;Corbett et al.,
153 1997;Dimova et al., 2015;Dimova and Burnett, 2011;Dimova et al., 2013;Kluge et al.,
154 2007;Kluge et al., 2012;Schmidt et al., 2010) and terrestrial rivers and streams

Deleted: studies utilize

Deleted: various methods including

Deleted: (Lee 1977, Shaw and Prepas 1990),

Deleted: (Gat 1995, Kluge et al. 2007, Kraemer 2005, Lazar et al. 2008),

Deleted: .

162 (Burnett et al., 2010;Cook et al., 2003;Cook et al., 2006;Batlle-Aguilar et al., 2014).
163 Of particular interest are investigations of temporal ^{222}Rn distribution in lakes, since it
164 can be used to quantify groundwater discharge and reflect the locally climatological
165 dynamics (Dimova and Burnett, 2011;Luo et al., 2016). Temporal radon variations
166 give high resolution estimates of groundwater discharge to lakes over diel cycles,
167 allowing evaluation of LGD and the associated chemical loadings. However, there has
168 been no study of radon-based groundwater discharge in mountainous proglacial lakes,
169 especially for those lakes in the QTP.

170 This study aims to investigate the groundwater surface water interactions for the
171 proglacial lake of Ximen Co, by estimating the LGD and evaluating the hydrologic
172 partitioning of the lake. LGD is estimated with ^{222}Rn mass balance model, and the
173 hydrologic partitioning of the lake is obtained with the three endmember model
174 coupling the mass balance of water, stable isotopes and Cl. Moreover, LGD derived
175 nutrients are estimated and the nutrient budgets of the lake are depicted. This study,
176 to our knowledge, makes the first attempt to quantify the LGD, hydrologic partition,
177 and groundwater borne nutrients of the proglacial lake in QTP and elsewhere via the
178 approach integrating multiple tracers. This study provides insights of hydrologic
179 partitioning in a typical mountainous proglacial lake under current climate condition
180 and reveals groundwater borne chemical loadings in this proglacial lake in QTP and

Deleted: Then,

Deleted: Finally, primary productivity of the lake water is calculated based on the nutrient budgets.

185 elsewhere.

186

187 **2. Methodology**

188 2.1 Site descriptions

189 The Nianbaoyeze MT., located at the eastern margin of the QTP and being the
190 easternmost part of NW-SW trending Bayan Har Shan, is situated at the main water
191 divide of the upper reaches of Yellow River and Yangtze River (Figure 1). With a peak
192 elevation of 5369 m, the mountain rises about 500-800 m above the surrounding
193 peneplain and displays typical Pleistocene glacial landscapes such as moraines,
194 U-shaped valleys and cirques (Lehmkuhl, 1998; Schlutz and Lehmkuhl,
195 2009; Wischnewski et al., 2014). The present snow line is estimated to be at an
196 elevation of 5100 m (Schlutz and Lehmkuhl, 2009). Controlled by the South Asia and
197 East Asia monsoons, the mountain has an annual precipitation of 975 mm in the
198 southern part and 582 mm in the northwestern part, with 80 % occurring during May
199 and October (Yuan et al., 2014; Zhang and Mischke, 2009). The average temperature
200 gradient is about 0.55 °C per 100 m, and the closest weather station, locating in Jiuzhi
201 town (N: 33.424614 °, E: 101.485998) at the lower plains of the mountain, recorded a
202 mean annual temperature of 0.1 °C. Snowfalls occur in nearly 10 months of the entire
203 year and there is no free-frost all year around (Böhner, 1996, 2006; Schlutz and

204 Lehmkuhl, 2009). The precipitation, daily bin-averaged wind speed and temperature
205 | in Aug, 2015 were recorded to be 90 mm, 0.7 m s^{-1} and $9.5 \text{ }^{\circ}\text{C}$ from Jiuzhi weather
206 station (Figure 2). The water surface evaporation was recorded to be 1429.8 mm in
207 2015 from Jiuzhi weather station.

208 Among the numerous proglacial lakes developed in the U-shaped valleys of the
209 Nianbaoyeze MT., Ximen Co lake is located at the northern margin of the mountain
210 with an elevation of 4030 m asl, and is well studied and easily accessible (Lehmkuhl,
211 1998;Zhang and Mischke, 2009;Schlutz and Lehmkuhl, 2009;Yuan et al., 2014). The
212 lake was formed in a deep, glacially eroded basin with a catchment area of 50 km^2 ,
213 and has a mean and a maximum depth of 40 m and 63.2 m, and a surface area of 3.6
214 km^2 . The vegetation around the lake is dominated by pine meadows with dwarf shrubs,
215 rosette plants and alpine cushion (Schlutz and Lehmkuhl, 2009;Zhang and Mischke,
216 2009;Yuan et al., 2014). Mostly recharged by the glacial and snowpack melting water
217 and regional precipitation, the lake is stratified with an epilimnion depth about 4.4 m
218 in the summer time. The lake is usually covered by ice in the winter time (Zhang and
219 Mischke, 2009). The superficial layer within the U-shaped valley is characterized by
220 peat, clay and fluvial gravels with a depth about 1-3.5 m. Discontinuous and isolated
221 permafrost is present at the slope of the valley above the elevation of about 4150 m.
222 The maximum frozen depth is about 1.5 m for the seasonal frozen ground around the

223 lake. The seasonal frozen ground serves as an unconfined aquifer during the unfrozen
224 months from July to October, and groundwater discharges into the epilimnion of the
225 lake (Wang, 1997; Schlutz and Lehmkuhl, 2009; Zhang and Mischke, 2009).

226

227 2.2 Sampling and field analysis

228 The field campaign to Ximen Co Lake was conducted [in](#) August, 2015, when it is
229 warm enough to take the water samples of different origins as the studied site is
230 seasonally frozen. A ²²²Rn continuous monitoring station was setup at the southeast

231 part of the lake, [where](#) is fairly flat for setting up our tent and monitoring system.

232 Surface water samples were collected around the lake, rivers at the upstream and
233 downstream. Porewater samples were collected at one side of the lake as the other
234 side is steep and rocky. The basic water quality parameters of conductivity (EC),
235 dissolved oxygen (DO), TDS, ORP, [and](#) pH in the water were recorded with the
236 multi-parameter meter (HANNA, Co.). Relative humidity was recorded with a
237 portable thermo-hydrometer (KTH-2, Co.). Lake water samples were taken with a
238 peristaltic pump into 2.5 L glass bottles for ²²²Rn measurement with the Big Bottle
239 system (Durrige, Co.). Surface water samples were filtered with 0.45 µm filters
240 (Advantec, Co.) in situ and taken into 5 ml, 15 ml, 15 ml and 50 ml Nalgene
241 centrifugation tubes for stable isotope, major anion, cation and nutrient analysis.

Deleted: from

Deleted: which

244 Porewater samples were taken from the lakes shore aquifers with a push point sampler
245 (M.H.E, Co.) connected to peristaltic pump (Solinst, Co.) (Luo et al., 2014;Luo et al.,
246 2016). 100 ml raw surface water or porewater was titrated with 0.1 μM H_2SO_4
247 cartridge (Hach, Co.) in situ to measure total alkalinity (Hasler et al., 2016;White et
248 al., 2016;Warner et al., 2013). Porewater was filtered with 0.45 μm syringe filters in
249 situ and taken into 5 ml, 15 ml, 15 ml and 50 ml Nalgene centrifugation tubes for
250 stable isotope, major anion, cation and nutrient analysis. 250 ml porewater was taken
251 for ^{222}Rn measurement with RAD7 H₂O (Durridge, Co.). Samples for major cation
252 analysis were acidified with distilled HNO_3 immediately after the sampling.

253 ^{222}Rn continuous monitoring station was set up at the northwest of the lake, close
254 to the downstream of the lake (Figure 1b). Lake water (about 0.5 m in depth) was
255 pumped with a DC pump (12 V) driven by lithium batteries (100 Ah) and sprinkled
256 into the chamber of RAD7 AQUA with a flow rate $> 2 \text{ L min}^{-1}$, where ^{222}Rn in water
257 vapor was equilibrated with the air ^{222}Rn . The vapor in the chamber was delivered
258 into two large dry units (Drierite, Co) to remove the moisture and circulated into
259 RAD7 monitor, where ^{222}Rn activities were recorded every 5 mins. A temperature
260 probe (HOBO[®]) was insert into the chamber to record the temperature of the water
261 vapor. The monitoring was performed from 11: 31 am, Aug 22nd to 6: 30 am, Aug 24th,
262 2015. During the period of 1:50-4:30 pm on Aug 22nd, a sudden blizzard occurred,

Deleted: (Advantec, Co.)

Deleted: L

265 leading to an hourly precipitation about 0.6 mm to the lake area. Daily and hourly
266 climatological data such as wind speed, air temperature and precipitation were
267 retrieved from the nearest weather station in Jiuzhi town (N: 33.424614 °, E:

268 101.485998). Moreover, another RAD7 was placed at the lakes hore to measure ²²²Rn
269 in the ambient air around the lake. Due to extremely low activities, the monitoring
270 period was conducted only for 4 hours, and the mean activity was adopted as the
271 background radon-222 activity to be used in the mass balance model. Water level and

272 temperature fluctuations were recorded with a conductivity-temperature-depth diver
273 (Schlumberger, Co.) fixed at about 20 cm below the lake surface and calibrated with
274 local atmospheric pressure recorded by a baro-diver (Schlumberger, Co.) above the
275 lake. To correct for dissolved ²²⁶Ra supported ²²²Rn, one radium sample was extracted
276 from 100 L lake water with MnO₂ fiber as described elsewhere (Luo et al.,
277 2014;Moore, 1976).

278

279 2.3 Chemical analysis

280 Major ions were measured with ICS-1100 (Dionex. Co.) in the Department of Earth
281 Sciences, the University of Hong Kong. The uncertainties of the measurements are
282 less than 5 %. Nutrients, DIN and DIP were analyzed with flow injection analysis
283 equipped with auto-sampler (Lachat. Co.) in the School of Biological Sciences, the

Deleted: monitor

Deleted: set

Formatted: Superscript

Deleted: s

Deleted: er

Deleted: when constructing

289 University of Hong Kong. Stable ^{18}O and ^2H isotopes were measured with
290 MOA-ICOS laser absorption spectrometer (Los Gatos Research (LGR) Triple Isotope
291 Water Analyzer (TIWA-45EP)) at State Key Laboratory of Marine Geology, Tongji
292 University, Shanghai. The stable isotopic standards and the recovery test have been
293 fully described elsewhere (Luo et al., 2017). The measurement uncertainty is better
294 than 0.1 % for ^{18}O and 0.5 % for ^2H . ^{226}Ra was detected with RAD7 with the method
295 described elsewhere (Kim et al., 2001; Lee et al., 2012; Luo et al., 2018).

Deleted: has

296

297 2.4 Radon transient model

298 Previous studies employed a steady state radon-222 mass balance model to
299 quantify LGD to lentic system such as lakes and wetlands (Dimova and Burnett,
300 2011; Luo et al., 2016). This model assumes that radon input derived from
301 groundwater inflow, diffusion and river inflow are balanced by the radon losses of
302 atmospheric evasion, decay and river outflow. However, recent studies revealed that
303 the steady state is mainly reached after 2-15 days of constant metrological conditions,
304 and most lentic system cannot be treated as steady state due to rapid radon-222
305 degassing to the atmosphere driven by wind-induced turbulence (Gilfedder et al.,
306 2015; Dimova and Burnett, 2011).

Deleted: ly

Deleted: ly

Deleted: be

307 Ximen Co lake is demonstrated to be highly stratified with an epilimnion of 4.4

312 m (Zhang and Mischke, 2009). The lake was formed by glacier erosion and the
313 lakebed is characterized by granite bedrock with a thin sedimentary clay layer.

314 Previous studies have indicated that sediment consisting of clay, soils and gravels, has
315 been developed on the bedrock and forms the lake shore aquifer with a thickness of
316 0.7-3.3 m (Schlutz and Lehmkuhl 2009). Porewater sampled in the aquifer immediate,

Deleted: with a thickness of 0.7-3.3 m

Deleted: , which consists of clay, soils and gravels

Deleted: ly

317 behind the lake shore can well represent groundwater discharging into the lake, as
318 suggested previously (Lewandowski et al., 2015; Rosenberry et al., 2015; Schafran and
319 Driscoll, 1993). LGD has been widely considered to occur within the first few meters
320 of the lake shore (Schafran and Driscoll, 1993; Rosenberry et al., 2015; Lee et al., 1980)
321 and groundwater is considered to predominately discharge into the epilimnion since
322 deep groundwater flow is highly limited by the Precambrian bedrock (Einarsdottir et

323 al., 2017). Due to negligible hydrological connection between the epilimnion and
324 hypolimnion, ²²²Rn mass balance model is established to quantify LGD to the
325 epilimnion from the lake shore.

Deleted: 2016

Deleted: Therefore,

Deleted: Due to negligible hydrological connection between the epilimnion and hypolimnion, LGD for the lake can be quantified with ²²²Rn mass balance model for the epilimnion.

326 The governing equation of radon-222 transient mass balance model within a 1 x
327 1 x z cm (where z is the depth in cm) can be expressed as (Gilfedder et al., 2015):

328
$$z \frac{\partial I_w}{\partial t} = F_{gw} + (I_{226Ra} - I_w) \times z \times \lambda_{222} + F_{diff} - F_{atm} \quad (1)$$

329 where F_{gw} , F_{diff} , F_{atm} [Bq m⁻² d⁻¹] are ²²²Rn loadings from LGD, water-sediment
330 diffusion and water-air evasion, respectively; z [m] is the lake water level depth

342 recorded by the diver. λ_{222} is the decay constant of ^{222}Rn with a value of 0.186 d^{-1} .
343 $\lambda_{222} \times I_{^{226}\text{Ra}}$ and $\lambda_{222} \times I_w$ account for the production and decay of ^{222}Rn [$\text{Bq m}^{-2} \text{ d}^{-1}$]
344 in the water column, respectively. I_w and $I_{^{226}\text{Ra}}$ [Bq m^{-2}] represent ^{222}Rn and ^{226}Ra
345 inventories in the epilimnion, and are expressed as: $I_w = H \times C_w$ and
346 $I_{^{226}\text{Ra}} = H \times C_{^{226}\text{Ra}}$, respectively; where H [m] is the depth of the epilimnion; C_w and
347 $C_{^{226}\text{Ra}}$ is the ^{222}Rn and ^{226}Ra activity [Bq m^{-3}], respectively.

348 The model is valid under the following assumptions: 1) The epilimnion is well
349 mixed which is the actual condition for most natural boreal and high altitude glacial
350 lakes (Zhang and Mischke, 2009; Åberg et al., 2010). 2) ^{222}Rn input from riverine
351 water inflow, and loss from the lake water outflow and infiltration into the lake shore
352 aquifer is negligible compared to the groundwater borne ^{222}Rn , because ^{222}Rn
353 concentration of groundwater is 2-3 orders of magnitude larger than that of lake water
354 (Dimova and Burnett, 2011; Dimova et al., 2013). Generally, ^{222}Rn in the epilimnion is
355 sourced from LGD and decay input from parent isotope of ^{226}Ra under secular
356 equilibrium, and is mainly lost via atmospheric evasion and radioactive decay.

357 F_{atm} is the key sinking component of the transient model and is finally a function of
358 wind speed and water temperature, both of which are temporal variant variables
359 (Supplementary information). Lake water level z is also a temporal variant variable
360 which represents the fluctuations of water volume of the epilimnion. This equation is

361 discretized by the forward finite difference method, and the groundwater flux at each
362 time step can be solved as follow

$$363 \quad [{}^{222}\text{Rn}_{t+\Delta t}] = \frac{[z \times {}^{222}\text{Rn}_t + [F_{diff} + F_{gw} - F_{atm} - {}^{222}\text{Rn}_t \times \lambda \times z] \times \Delta t}{z} \quad (2)$$

364 where ${}^{222}\text{Rn}_{t+\Delta t}$ and ${}^{222}\text{Rn}_t$ [Bq m⁻³] is the ²²²Rn activity at current time step and at

365 the previous time steps, respectively, and Δt [min] is the time step which is set to be

366 5 min in consistence with the ²²²Rn record interval. With the inverse calculation based

367 on Equation (2), the groundwater inflow at each time step can be obtained. However,

368 large errors of the final LGD calculation will be induced by even a small amount of

369 noise in the measured ²²²Rn data due to the ${}^{222}\text{Rn}_{t+\Delta t} - {}^{222}\text{Rn}_t$ term being with the

370 measure uncertainty. To reduce the random errors of the measured ²²²Rn

371 concentrations, the time window with a width of 1 hour is proposed to smooth the

372 curve (Supplementary information).

373

374 3. Results

375 3.1 Time series data

376 Figure 2 shows the basic climatological parameters of the lake catchment during

377 the campaign month. There are discrete rainfall events occurring throughout the

378 month with an average rainfall of 3.1 mm d⁻¹. The temperature during the month

379 ranges from 5.0 – 12.5 °C within an average of 9.3 °C. The daily averaged wind speed

380 ranges from 0.7 – 2.5 m s⁻¹, with an average of 1.7 m s⁻¹. ²²²Rn temporal distribution

Formatted: Superscript

Deleted: 4

Deleted: throughout

Deleted: generally

384 and other time series data are shown in Figure 3a and listed in Supplementary Table 1.
385 Generally, ^{222}Rn concentration varies from 32.2 to 273 Bq m^{-3} , with an average of
386 $144.2 \pm 27.7 \text{ Bq m}^{-3}$. ^{222}Rn over the monitoring period shows typical diel cycle, much
387 higher at nighttime and lower in the day time. Figures 3b-3d show the time series data
388 of temperature (5 mins interval), nearshore lake water level (1 min interval), and wind
389 speed (1 hour interval). Temperature and lake water level also show typical diel cycles,
390 but with antiphase fluctuations with each other. Temperature is higher during the
391 daytime and lower at nighttime. However a sudden decrease of temperature was
392 recorded due to the sudden blizzard (Figure 3b). Water level is higher at nighttime and
393 lower during the daytime, with a strong fluctuation due to the turbulence caused by
394 the blizzard (Figure 3c). The variability might reflect the dynamics of groundwater
395 input and surface water inflow. The air temperature of the lake area is in phase with
396 the water temperature. Wind speed is normally higher during the daytime and lower at
397 nighttime (Figure 3d).

398 The variation of ^{222}Rn is nearly in antiphase with the fluctuations of lake water
399 temperature and air temperature, indicating that the dominated controlling factors of
400 ^{222}Rn fluctuations are water temperature and wind speed (Figure 3a). This
401 phenomenon is reasonable as lake water ^{222}Rn is predominately lost via atmospheric
402 evasion, which is the function of wind speed and water temperature (Dimova et al.,

Deleted: s

404 2015;Dimova and Burnett, 2011;Dimova et al., 2013). High water temperature and
405 wind speed leads to elevated atmospheric evasion and causes the decline of ^{222}Rn
406 concentration in the lake water. However, there is a sudden reduction of radon activity
407 from 2: 00 pm to 4: 00 pm on Jul 22nd, 2015, when the snow event led to a sudden
408 decrease of water temperature, increase of wind speed, and large surface water
409 turbulence as indicated by water level fluctuations (Figures 3a-3d). ^{222}Rn in the
410 porewater is 2-3 orders of magnitude larger than ^{222}Rn in the lake water, suggesting
411 that ^{222}Rn is an ideal tracer to estimate the LGD (Supplementary Table 1). ^{222}Rn
412 concentrations in surface water range from 22.2 to 209 Bq m^{-3} , with an average of
413 92.5 Bq m^{-3} ($n = 12$), which is in the range of ^{222}Rn continuous monitoring results,
414 suggesting reliable ^{222}Rn measurements (Supplementary Table 2).

415

416 3.2 Geochemical results

417 The results of major ions, nutrients and stable isotopes in different water
418 endmembers are shown in Figures 4 and 5. Cl^- ranges from 0.6 to 2.1 mg L^{-1} in the
419 surface water (including riverine inflow water, lake water and downstream water), 0.4
420 to 2.7 mg L^{-1} in porewater and has a much higher concentration of 5.9 mg L^{-1} in
421 rainfall water. Na^+ ranges from 1.6 to 3.4 mg L^{-1} in the surface water, 1.2 to 4.4 mg
422 L^{-1} in porewater and has a concentration of 4.4 mg L^{-1} in rainfall water. SO_4^{2-} ranges

Deleted:

424 from 1.2 to 2.3 mg L⁻¹ in the surface water, 0.4 to 1.7 mg L⁻¹ in porewater and has a
425 significant low concentration of 0.01 mg L⁻¹ in rainfall water. Ca²⁺ ranges from 3.0 to
426 12.4 mg L⁻¹ in lake water, 3.4 to 12.5 mg L⁻¹ in porewater and has a significant^{ly} high
427 concentration of 20.5 mg L⁻¹ in rainfall water. Other concentrations of major ions are
428 listed in Supplementary Table 2. As shown in Figure 4d and Supplementary Table 2,
429 δ¹⁸O in the lake water ranges from - 13.06 ‰ to - 12.11 ‰, with an average of -
430 12.41 ‰ (n = 7), and δ²H ranges from - 91.83 ‰ to - 87.47 ‰, with an average of -
431 89.0 ‰ (n = 7). δ¹⁸O in the riverine inflow water ranges from - 13.44 ‰ to - 13.29 ‰,
432 with an average of - 13.37 ‰ (n = 2), and δ²H ranges from - 93.25 ‰ to - 91.92 ‰,
433 with an average of - 92.59 ‰ (n = 2). δ¹⁸O in the downstream water ranges from -
434 12.51 ‰ to - 12.18 ‰, with an average of - 12.35 ‰ (n = 3), and δ²H ranges from -
435 88.96 ‰ to - 87.1 ‰, with an average of - 87.98 ‰ (n = 3). δ¹⁸O in the porewater
436 ranges from - 12.66 ‰ to - 11.52 ‰, with an average of - 11.97 ‰ (n = 8), and δ²H
437 ranges from - 91.3 ‰ to - 82.87 ‰, with an average of - 85.5 ‰ (n = 8). DIN in the
438 surface water (including riverine inflow water, lake water and downstream water)
439 ranges from 6.6 to 16.9 μM, with an average of 10.3 μM, and DIP from 0.36 to 0.41
440 μM, with an average of 0.38 μM. DIN for the porewater ranges from 0.7 to 358.8 μM,
441 with an average of 92.8 μM, and DIP from 0.18 to 0.44 μM with an average of 0.31
442 μM (Figure 5).

Deleted: The concentrations of

444

445 4. Discussion

446 4.1 Proglacial hydrologic processes and geochemical implications

447 Generally, major ion concentrations in the lake water and porewater of Ximen

448 Co lake are significantly lower than those in major rivers, streams and other tectonic

Deleted: main

449 lakes in the QTP (Yao et al., 2015;Wang et al., 2010;Wang et al., 2016b), and are

450 similar to those of snow and glaciers (Liu et al., 2011), suggesting that the lake water

451 is mainly originated from glacier and snow melting. Ion concentrations in the lake and

452 porewater of Ximen Co lake are much lower than those of rainfall collected in Jiuzhi

453 town. This suggests that lake water is less influenced by precipitation (Figures 4a-4c).

454 The concentrations of major ions in the porewater are high compared to the lake water,

455 indicating weathering affects from the aquifer grains. The ratios of Ca^{2+}/Na^{+} in the

456 porewater and groundwater is >1 , also suggesting influences of weathering digenesis

457 of major ions from the seasonal frozen ground at the lake shore aquifer (Weynell et al.,

458 2016;Yao et al., 2015;Wang et al., 2010).

459 The isotopic compositions of the lake water and porewater are significantly

460 isotopically depleted, with values close to the compositions of glaciers and surface

461 snow in the QTP, suggesting the lake is dominantly recharged from snow and glacier

462 melting (Cui et al., 2014;Wang et al., 2016a;Zongxing et al., 2015). The relation of

464 $\delta^{18}\text{O}$ versus $\delta^2\text{H}$ for the lake water is $\delta^2\text{H} = 4.25 \times \delta^{18}\text{O} - 35.99$, with a slope much
465 lower than that of the global meteoric water line (GMWL) (Figure 4d), suggesting the
466 effects of lake surface evaporation. The relation of $\delta^{18}\text{O}$ versus $\delta^2\text{H}$ for the porewater
467 is $\delta^2\text{H} = 6.93 \times \delta^{18}\text{O} - 2.67$, overall on GMWL (Figure 4d). Deuterium excesses is
468 defined as $\Delta\text{D} = \delta\text{D} - 8 \times \delta^{18}\text{O}$ (Dansgaard, 1964). The value of ΔD is dependent on
469 air mass origins, altitude effect and the kinetic effects during evaporation (Hren et al.,
470 2009). Global meteoric water has a ΔD of + 10 ‰. In [the](#) QTP, glacier/snowpack
471 melting water usually has large positive ΔD , while the precipitations derived from
472 warm and humid summer monsoon has lower ΔD (Ren et al., 2017; Ren et al., 2013).

473 In this study, ΔD of surface water, lake and porewater ranges from + 8.5 to + 11.8 ‰,
474 closed to the glacier melting water but much smaller than that of the local
475 precipitation of + 18.8 ‰. This indicates the stream and lake water are mainly
476 originated from glacial/snowpack melting rather than precipitation (Gat, 1996; Wang
477 et al., 2016a; Lerman et al., 1995). The slopes of $\delta^2\text{H}$ versus $\delta^{18}\text{O}$ in lake water and
478 porewater are 4.25 and 6.93, both of which are lower than that of GMWL due to
479 surface evaporation. Lake water is more intensively influenced by evaporation
480 compared to porewater. The plots of $\delta^{18}\text{O}$ versus Cl^- , and $\delta^2\text{H}$ versus Cl^- are well
481 clustered for porewater end member (orange area), lake water end member (blue area),
482 riverine inflow water end member (yellow area), and precipitation water (Figures 4e

Deleted: 37.1

Deleted: 41.2

Deleted: larger

Deleted: 29.72

Deleted: ^{18}O

488 and 4f), suggesting stable $\delta^{18}\text{O}$ and $\delta^2\text{H}$ isotopes and Cl^- can serve as tracers to
489 quantify the hydrologic partitioning of the lake by setting three endmember models.

490 The concentrations of DIN and DIP are all within the ranges of other glacial
491 melting water and proglacial lake water (Hawkings et al., 2016;Hodson, 2007;Hudson
492 et al., 2000;Tockner et al., 2002;Hodson et al., 2005). Briefly, rainfall and upstream

493 lake water such as YN-4 have the highest DIN concentrations, indicating the glacier
494 melting and precipitation could be important DIN sources in proglacial areas
495 (Dubnick et al., 2017;Anderson et al., 2017). DIN in porewater is overall higher
496 compared to the lake water, suggesting the porewater to be DIN effective source; and

497 DIP concentration is higher in the lake water compared to porewater, suggesting the
498 porewater is a DIP sink (Figure 5). The N: P ratios in the lake water and porewater are

499 averaged to be 27.1 and 320.5, respectively, both much larger than the Redfield Ratio
500 (N: P = 16:1) in water and organism in most aquatic system and within the range of
501 other proglacial lakes (Anderson et al., 2017). This also suggests that the lake water
502 and porewater are under phosphate limited condition. N: P ratio in the rainfall water is

503 30.4, similar to the lake water. The average N: P ratio of porewater is much higher
504 than that of lake water, indicating DIN enrichment in the lake shore aquifers (Figure

505 5). In pristine groundwater, NO_3^- is the predominated form of dissolved nitrogen and
506 is highly mobile within the oxic aquifers, leading to much higher DIN concentrations

Deleted: has

Deleted: s

Deleted: N

510 in the porewater; DIP has high affinity to the aquifer grains, resulting in much lower
511 DIP concentrations in the porewater (Lewandowski et al., 2015; Rosenberry et al.,
512 2015; Slomp and Van Cappellen, 2004). Thus, in analogous to surface runoff from
513 glacier/snowpack melting, LGD can be also regarded as an important [DIN](#) source for
514 the proglacial lakes. Because of very high DIN and N: P ratios in the porewater, a
515 relatively small portion of LGD delivers considerable nutrients into the glacial lake,
516 shifting the aquatic N: P ratios and affecting the proglacial aquatic ecosystem
517 (Anderson et al., 2017).

518

519 4.2 Estimation of LGD

520 Figure 6a shows all the sinks and sources of radon with the epilimnion of the lake.
521 Within ^{222}Rn transient mass balance model, the dominant ^{222}Rn loss is atmospheric
522 degassing/evasion. Generally, ^{222}Rn degassing rate is the function of the radon-222
523 concentration gradient at the water-air interface and the parameter of gas piston
524 velocity k , which is finally the function of wind speed and water temperature (Dimova
525 and Burnett, 2011; Gilfedder et al., 2015). To evaluate ^{222}Rn evasion rate, this study
526 employs the widely used method proposed by MacIntyre et al. (1995) which is also
527 detailed described in [supplementary information](#). Based on the field data of ^{222}Rn
528 concentration in the lake water, wind speed and temperature log, the radon degassing

Deleted: Supplementary

Deleted: Information

531 rate is calculated in a range of 0.8 to 265.2 Bq m² d⁻¹, with an average 42.0 of Bq m²
532 d⁻¹.

533 In addition to the atmospheric loss and sedimentary diffusion inputs, ²²²Rn is also
534 sinked via radioactive decay, and sourced from decay of parent isotope of ²²⁶Ra. The
535 decay loss of ²²²Rn fluctuates in phase with the distribution of ²²²Rn concentration
536 monitored by RAD 7 AQUA. The equations to estimate benthic fluxes are shown in
537 supplementary information. The decay loss is calculated to be 26.4 to 223.4 Bq m⁻² d⁻¹,
538 with an average of 118.0 ± 22.7 Bq m⁻² d⁻¹. ²²⁶Ra concentration is 0.01 Bq m⁻³ for the
539 lake water. Under secular equilibrium, the ²²⁶Ra decay input can be calculated by
540 multiplying ²²⁶Ra concentration in the lake water with λ₂₂₂ (Corbett et al., 1997; Kluge
541 et al., 2007; Luo et al., 2016). ²²⁶Ra decay input is calculated to be 0.83 Bq m⁻² d⁻¹,
542 which is significantly low compared to other ²²²Rn sources to the epilimnion.

543 With the obtained sinks and sources of ²²²Rn in the lake, and the constants given in
544 Table 1, LGD rate can be obtained by dividing the groundwater derived ²²²Rn with its
545 concentration in groundwater endmember. The obtained LGD rate, ranges from -23.7
546 mm d⁻¹ to 90.0 mm d⁻¹, with an average of 10.3 ± 8.2 mm d⁻¹ (Figure 7). The LGD
547 rate range is relatively smaller than the daily lake water level variations (≈ 50 mm),
548 indicating that the lake water level variation could be a combined effect of surface
549 runoff and LGD (Hood et al., 2006). The negative values of LGD rate reflect the

Deleted: less

Deleted: s

551 return groundwater flow due to infiltration into the porewater. Normally, the
552 dominant values are positive, indicating LGD rate is significant compared to water
553 infiltration into lake shore aquifer. The temporal variation of LGD rate could be
554 attributed to the fluctuations of the hydraulic gradient in the proglacial areas (Hood et
555 al., 2006; Levy et al., 2015). As indicated by ΔD (mostly > 10) of surface water, the
556 lake and the upstream water is considered to be mainly recharged from
557 glacial/snowpack melting rather other precipitations.

558 To assess the magnitude of uncertainty of ^{222}Rn transient model, the sensitivity of
559 estimated LGD to changes in other variables is examined. A sensitivity coefficient f is
560 proposed to evaluate this uncertainty according to Langston et al. (2013)

$$561 \quad f = (\Delta F_{LGD} / F_{LGD}) / (\Delta y_i / y_i) \quad (3)$$

562 where ΔF_{LGD} is the amount of change in F_{LGD} from the original value. Δy_i is the
563 amount of change in the other variable of y_i from the original value. Thus, higher f
564 indicates a large uncertainty of final LGD estimate. The uncertainty mainly stems
565 from ^{222}Rn measurements in different water endmembers, the atmospheric loss and
566 water level record. The uncertainties of ^{222}Rn measurement are about 10 % and 15-20
567 % in groundwater and lake water endmember, respectively. The uncertainty of
568 atmospheric loss is derived from uncertainty of ^{222}Rn in lake water (with an
569 uncertainty of 15-20 %), temperature (with an uncertainty ≈ 5 %) and wind speed

571 (with an uncertainty $\approx 5\%$). Thus, the final LGD estimate has an [integrated](#)
572 uncertainty of 35-40 %.

573

574 **4.3 Hydrologic partitioning**

575 Compared to the groundwater labeled radionuclide of ^{222}Rn , stable $^{18}\text{O}/^2\text{H}$
576 isotopes are advantageous in the investigation of evaporation processes due to their
577 fractionations from water to vapor and have been widely used to investigate the
578 hydrologic cycle of lakes in various environments (Stets et al., 2010; Gat,
579 1995; Gonfiantini, 1986; Gibson et al., 1993). With the field data of stable isotopic
580 composition and Cl^- concentrations in different water endmembers, groundwater input,
581 surface water input, lake water outflow and infiltration, and evaporation can be
582 partitioned by coupling stable isotopic mass balance model with Cl^- mass balance
583 model (Figure 6b).

584 The model, consisting of the budgets of stable isotopes and Cl^- , and water masses
585 for the epilimnion, is used to quantify riverine inflow, lake water outflow and
586 infiltration, and evaporation (LaBaugh et al., 1995; LaBaugh et al., 1997; Gibson et al.,
587 2016). The model is valid under the following assumptions: (1) constant density of
588 water; (2) no long-term storage change in the reservoir; (3) well-mixed for the
589 epilimnion (Gibson, 2002; Gibson et al., 2016; Gibson and Edwards, 2002; LaBaugh et

Deleted:

591 al., 1997). The above assumptions are reasonably tenable during the short monitoring
 592 period. The model can be fully expressed as

$$593 \quad F_{in} + F_{LGD} + F_p = F_E + F_{out} \quad (4)$$

$$594 \quad F_{in} \times \delta_{in} + F_{LGD} \times \delta_{gw} + F_p \times \delta_p = F_E \times \delta_E + F_{out} \times \delta_L \quad (5)$$

$$595 \quad F_{in} \times [Cl^-]_{in} + F_{LGD} \times [Cl^-]_{gw} + F_p \times [Cl^-]_p = F_E \times [Cl^-]_L + F_{out} \times [Cl^-]_p \quad (6)$$

596 where F_{in} [mm d⁻¹] is the surface water inflow to the lake; F_{gw} [mm d⁻¹] is LGD rate.

597 F_p [mm d⁻¹] is the mean daily rainfall rate during the sampling period. F_E [mm d⁻¹] is

598 the lake evaporation. F_{out} [mm d⁻¹] is the lake water outflow via runoff and

599 infiltration into the lake shore aquifer. δ_{in} , δ_{gw} , δ_E and δ_p are the isotopic compositions

600 of surface water inflow, LGD, and evaporative flux, respectively. The values of δ_{in} ,

601 δ_{gw} and δ_p are obtained from field data and the composition of δ_E are calculated as

602 shown in supplementary information. $[Cl^-]_{in}$, $[Cl^-]_{gw}$, $[Cl^-]_L$ and $[Cl^-]_p$ are the

603 chloride concentrations in the inflow water, porewater, lake water and precipitation,

604 respectively.

605 The components of the mass balance model can be obtained from the field data of

606 isotopic composition and Cl⁻ concentrations in different water endmembers. The

607 average ¹⁸O composition -13.37 ‰ of riverine inflow water is taken as the value of

608 the input parameter δ_{in} . $\delta^{18}O$ and δ^2H in the groundwater endmember and lake water

609 end member are calculated to be -12.41 ‰ and -87.18 ‰, respectively. $\delta^{18}O$ and δ^2H

Deleted: .

611 in the rainfall are measured to be -5.47 ‰ and -24.98 ‰, respectively. With the
612 measured values of δ_L , h , δ_m , and the estimated ε and δ_a , the isotopic composition
613 of δ_E is calculated to be -35.11 ‰, which is in line with the results of alpine and
614 arctic lakes elsewhere (Gibson, 2002;Gibson et al., 2016;Gibson and Edwards, 2002).
615 The values of $[Cl^-]_{in}$, $[Cl^-]_{gw}$, and $[Cl^-]_L$ are calculated to be 0.91 mg L⁻¹, 1.48
616 mg L⁻¹ and 1.02 mg L⁻¹, respectively. All the parameters used in the model are shown
617 in Table 2.

618 According to Equations 4-6, the uncertainties of calculations of F_{in} , F_{out} and E are
619 mainly derived from the uncertainty of F_{LGD} and the compositions of Cl⁻, δD and $\delta^{18}O$
620 in different water endmembers as suggested in previous studies (Genereux,
621 1998;Klaus and McDonnell, 2013). The compositions of Cl⁻, δD and $\delta^{18}O$ in surface
622 water, groundwater endmembers have an uncertainty of 5 %. The uncertainty of δ_E is
623 reasonably assumed to be ≈ 20 %. Thus, considering the uncertainty propagation of
624 all the above parameters, the uncertainties of F_{in} , F_{out} and E would be scaled up to
625 70-80 % of the final estimates.

626

627 4.4 The hydrologic partitioning of the glacial lake

628 Based on the three endmember model of ^{18}O and Cl⁻, the riverine inflow rate was
629 calculated to be 135.6 ± 119.0 mm d⁻¹, and the lake outflow rate is estimated to be

630 141.5 ± 132.4 mm d⁻¹; the evaporation rate is calculated to be 5.2 ± 4.7 mm d⁻¹. The
631 summary of the hydrologic partitioning of the lake is shown in Figure 8a. Generally,
632 the proglacial lake is mostly recharged by the riverine inflow from the snowpack or
633 the glacier melting. The groundwater discharge contributes about only 7.0 % of the
634 total water input to the lake, indicating groundwater input does not dominate water
635 input to the proglacial lake. The recent review on LGD rate by Rosenberry et al.
636 (2015) suggests that the median of LGD rate in the literatures is 7.4 mm d⁻¹ (0.05 mm
637 d⁻¹ to 133 mm d⁻¹), which is about 2/3 of LGD rate in this study. This difference may
638 be due to the hydrogeological setting of the lake shore aquifer. This aquifer is formed
639 by grey loam, clayey soil and sand (Lehmkuhl, 1998; Schlutz and Lehmkuhl, 2009),
640 which is with relatively high permeability.

641 Previous studies have indicated that groundwater forms a key component of
642 proglacial hydrology (Levy et al., 2015). However, there have been limited
643 quantitative studies of groundwater contribution to hydrologic budget of proglacial
644 areas. This study further summarizes the groundwater discharge studies over the
645 glacial forefield areas. Based on long term hydrological and climatological parameter
646 monitoring on the Nam Co lake in the QTP, Zhou et al. (2013) estimated the LGD to
647 be 5-8 mm d⁻¹, which is comparable to the surface runoff input and LGD of this study.
648 Brown et al. (2006) investigated the headwater streams at the proglacial areas of

Deleted: The lake water is mainly lost via surface water outflow and infiltration to the lake shore aquifers. The evaporation constitutes relatively small ratio (≈ 3.5 %) of total water losses. The annual evaporation rate was recorded to be 1429.8 mm (equivalent to 3.92 mm d⁻¹) in 2015 by the Jiuzhi weather station, lower than the obtained evaporation in this study. This may be due to much higher evaporation in August during the monitoring period.

Formatted: Font color: Red

Formatted: Font color: Red

Deleted: Brown et al. (2006), (Zhou et al. 2013)

Formatted: Superscript

662 Taillon Glacier in French and found that groundwater contributes 6-10 % of the
663 stream water immediate downwards of the glacier. Using water mass balance model,
664 Hood et al. (2006) shows that groundwater inflow is substantial in the hydrologic
665 partitioning of the proglacial Lake O'Hara in front of Opabin Glacier in Canada and
666 comprised of 30 -74 % of the total inflow. Roy and Hayashi (2008) studied the
667 proglacial lakes of Hungabee lake and Opabin lake at glacier forefield of Opabin
668 Glacier and found that groundwater component is predominant water sources of the
669 lakes and consisted of 35-39 % of the total water input of the lakes. Langston et al.
670 (2013) further investigated a tarn immediate in front of Opabin Glacier and indicated
671 the tarn is predominantly controlled by groundwater inflow/outflow, which consisted
672 of 50-100 % of total tarn volume. Magnusson et al. (2014) studied the streams in the
673 glacier forefield of Dammagletscher, Switzerland and revealed that groundwater
674 contributed only 1-8 % of the total surface runoff. Groundwater contribution in this
675 study is similar to those obtained the mountainous proglacial areas in Europe, but
676 much lower than those obtained in the proglacial areas of polar regions. It is
677 concluded that proglacial lakes/streams in front of mountainous glaciers are mainly
678 recharged by surface runoff from glacier/snowpack melting. This might be due to
679 well-developed stream networks and limited deep groundwater flow (Einarsdottir et
680 al., 2017;Brown et al., 2006;Magnusson et al., 2014). However, proglacial tarns and

681 lakes in the polar areas are predominantly controlled by groundwater discharge, due
682 to less connectivity of surface runoff and high shallow and deep groundwater
683 connectivity (Langston et al., 2013; Hood et al., 2006; Roy and Hayashi, 2008).

684 The evaporation constitutes relatively small ratio ($\approx 3.5\%$) of total water losses. The
685 annual evaporation rate was recorded to be 1429.8 mm (equivalent to 3.92 mm d^{-1}) in
686 2015 by the Jiuzhi weather station, lower than the obtained evaporation in this study.
687 This may be due to much higher evaporation in August during the monitoring period.

688 The estimation of evaporation in this study generally represents the upper limit of the
689 lake, as the sampling campaign was conducted during the summer time when the
690 highest evaporation might occur. The lake surface evaporation derived from the pan
691 evaporation in the QTP ranges from $\sim 700\text{ mm yr}^{-1}$ in the eastern QTP to over 1400
692 mm yr^{-1} in the interior lakes of the QTP (Zhang et al., 2007; Ma et al., 2015; Yang et
693 al., 2014). The evaporation of this study is rather in line with the previous evaporation
694 observation in the eastern QTP, stressing the tenability of evaporation in this study.

695 The runoff input is predominated recharge component ($> 90\%$) compared to other
696 components, with an area normalized value comparable to previous studies of runoff
697 input in other glacial melting dominant lakes in the QTP (Zhou et al., 2013; Zhang et
698 al., 2011; Biskop et al., 2016). The runoff input and the lake evaporation of the study
699 area, however, are subject to highly daily, seasonal and inter-annual variability as

Deleted: The lake water is mainly lost via surface water outflow and infiltration to the lake shore aquifers.

Formatted: Indent: First line: 0 ch

Deleted: ese studies

Deleted: s

Deleted: Eastern QTP

Deleted: is

Deleted: over

Deleted: \approx

Formatted: Superscript

Formatted: Superscript

Deleted: e

710 [indicated by previous studies in the QTP \(Zhou et al., 2013;Lei et al., 2017;Ma et al.,](#)
711 [2015;Lazhu et al., 2016\)](#). [Therefore, further investigations of long term and high](#)
712 [resolution climatological and isotopic data are required to provide precise constraints](#)
713 [of hydrologic partitioning of the lakes in the QTP,](#)

Deleted: es

Deleted: (Ma et al. 2015, Zhang et al. 2007)(Zhang et al. 2013)

Formatted: Font color: Red

Deleted: .

714 4.5 LGD derived nutrient loadings, nutrient budget and ecological implications

715 Compared to extensive studies of SGD derived nutrient loadings in the past decade
716 (Luo and Jiao, 2016;Slomp and Van Cappellen, 2004), studies of LGD derived
717 nutrient loadings have received limited attention, even given the fact that groundwater
718 in lake shore aquifers is usually concentrated in nutrients (Lewandowski et al.,
719 2015;Rosenberry et al., 2015). Even fewer studies focus on chemical budgets in the
720 proglacial lakes which are often difficult to access for sampling. Groundwater borne
721 DIN and DIP across the sediment-water interface in this study are determined with an
722 equation coupling the advective or LGD-derived, and diffusive solute transport
723 (Lerman et al., 1995;Hagerthey and Kerfoot, 1998)

724
$$F_j = -nD_j^m \frac{dC_j}{dx} + v_{gw} C_j \quad (7)$$

725 where $-nD_j^m \frac{dC_j}{dx}$ is the diffusion input and $v_{gw} C_j$ is the LGD derived fluxes, F_j
726 [$\mu\text{M m}^{-2} \text{d}^{-1}$] is the mol flux of nutrient species j (representing DIN or DIP). n is the
727 sediment porosity. D_j^m is the molecular diffusion coefficient of nutrient species j ,

732 which is given to be $4.8 \times 10^{-5} \text{ m}^2 \text{ d}^{-1}$ for DIP (Quigley and Robbins, 1986), and $8.8 \times$
733 $10^{-5} \text{ m}^2 \text{ d}^{-1}$ for DIN (Li and Gregory, 1974), respectively. C_j [μM] is the
734 concentration of nutrient species j . x [m] is the sampling depth. v_{gw} is LGD rate
735 estimated by ^{222}Rn mass balance model and has a value of $10.3 \pm 8.2 \text{ mm d}^{-1}$. $\frac{dC_j}{dx}$ is
736 the concentration gradient of nutrient species j across the water-sedimentary interface.

737 Substituting the constants and the field data of DIN and DIP in to Equation 6, LGD
738 derived nutrient loadings are calculated to be $954.3 \mu\text{mol m}^{-2} \text{ d}^{-1}$ and $3.2 \mu\text{mol m}^{-2} \text{ d}^{-1}$
739 for DIN and DIP, respectively. Riverine inflow brings $1195.0 \mu\text{mol m}^{-2} \text{ d}^{-1}$ DIN, 52.9
740 $\mu\text{mol m}^{-2} \text{ d}^{-1}$ DIP into the lake. Lake water outflow derived nutrient loss is estimated
741 to be $1439.9 \mu\text{mol m}^{-2} \text{ d}^{-1}$ and $54.7 \mu\text{mol m}^{-2} \text{ d}^{-1}$ for DIN and DIP, respectively.
742 Nutrients in the lake can be also sourced from atmospheric deposit (mostly in form of
743 precipitation). With the nutrient concentrations in the rain water during the monitoring
744 period, the wet deposit is calculated to be $76 \mu\text{mol m}^{-2} \text{ d}^{-1}$ and $2.5 \mu\text{mol m}^{-2} \text{ d}^{-1}$, for
745 DIN and DIP, respectively. The loadings of DIN to the lakes are mainly from surface
746 runoff and LGD, which comprised of 42.9 % and 53.7 % of the total DIN loadings.
747 Groundwater derived DIP input, however, constitutes only 6.3 % of the total DIP
748 inputs to the lake, indicating groundwater borne DIP is less contributive to the
749 nutrient budget of the lake compared to DIN. Very recent studies on polar regions
750 have indicated that the glacier/snowpack water is the main N sources to the proglacial

Deleted:..

752 lakes (Anderson et al., 2013;Dubnick et al., 2017). However, they do not consider the
753 contribution of groundwater borne N, in spite of the high groundwater connectivity in
754 the proglacial areas (Roy and Hayashi, 2008). This study stresses that groundwater
755 borne DIN could be comparable to the surface runoff derived DIN.

756 Based on nutrient results, the lake is considered to be an oligotrophic lake, similar
757 to other glacier melting dominant lakes in the OTP (Mitamura et al., 2003;Liu et al.,
758 2011). Phytoplankton is good dissolved organic phosphate (DOP) recyclers and will
759 overcome inorganic P limitation though DOP cycling in most template lakes (Hudson
760 et al., 2000). However, this may be not applicable for the glacial melting water and
761 the peri/pro-glacial lake water. Previous studies show that phosphate nutrients are
762 dominated by DIP and particulate phosphate, and the DOP contributes less than 10 %
763 of the dissolved phosphate (Cole et al., 1998;Hawkings et al., 2016;Hodson, 2007).
764 Thus DOP recycling is not likely to low N: P ratio under these conditions. Thus, the
765 primary production (PP) is therefore considered to be controlled by the DIP loadings.
766 The sum of DIN and DIP inputs minus the calculated DIN and DIP outputs leads to
767 surpluses of 785.4 $\mu\text{mol m}^{-2} \text{d}^{-1}$ and 3.9 $\mu\text{mol m}^{-2} \text{d}^{-1}$ for DIN and DIP, respectively.
768 The surpluses are expected to be consumed by the phytoplankton and converted into
769 the PP under phosphate limited conditions. As primary producers in the fresh
770 lacustrine system consume the nutrient under variant N: P ratios (7.1 to 44.2, mean:

Deleted: elsewhere

Deleted: and under phosphate limited condition

Moved down [1]: Thus, the primary production (PP) is therefore considered to be controlled by the DIP loadings. The sum of DIN and DIP inputs minus the sum of the calculated DIN and DIP outputs leads to surpluses of 785.4 $\mu\text{mol m}^{-2} \text{d}^{-1}$ and 3.9 $\mu\text{mol m}^{-2} \text{d}^{-1}$ for DIN and DIP, respectively.

Deleted: d

Field Code Changed

Deleted: ?

Deleted: ?

Deleted: is?

Field Code Changed

Deleted: are

Deleted: er

Deleted: The surpluses are expected to be consumed by the phytoplankton and converted into the PP under the Red Field ratio (C: N: P = 106: 16: 1), leading to a PP of 0.41 $\text{mmol C m}^{-2} \text{d}^{-1}$.

Moved (insertion) [1]

Deleted: ?

Deleted: difference between the

Deleted: sum of

Deleted: and

Deleted: minus

Deleted: sum of the

Field Code Changed

Formatted: Superscript

Deleted: The

Formatted: Font: Times New Roman

Formatted: Superscript

Deleted: are

Deleted: as summarized

Deleted: The estimated primary productivity is lower than most temperate eutrophicated and ologotrophic lakes (Cole et al. 1998, Smith 1979), and comparable to some high latitude or altitude lakes (Richerson et al. 1986, Sterner 2010).

798 [22.9](#)) (Downing and McCauley, 1992), [the biological uptake of DIN is roughly](#)
799 [estimated to be \$89.3 \mu\text{M m}^2 \text{d}^{-1}\$. Therefore, the nutrient budgets for DIN and DIP](#)
800 [can be finally conceptualized](#) in Figures 8b and 8c.

801 4.6. Implications, prospective and limitations

802 Mountainous proglacial lakes are readily developed in glacier forefields of QTP and
803 other high mountainous glacial such as Europe Alps and Pamir at central Asian
804 (Heckmann et al. 2016). The proglacial lakes are always trapping system of sediment
805 and sinks for water and chemical originated from glacier/snowpack melting and
806 groundwater. In analogous to cosmogenic isotopes such as ^{10}Be serving as a tool to
807 quantify the sediment sources, approaches integrating ^{222}Rn and stable isotopes
808 provides both qualitatively and quantitatively evaluations of groundwater
809 contributions and hydrologic partitioning in these remote and untapped lacustrine
810 systems. Thus, it is expected that the multiple aqueous isotopes is considered to be
811 effective tools to investigate the LGD and hydrologic partitioning in other proglacial
812 lakes. This study is mainly limited by the relatively short sampling and monitoring
813 period. As a special hydrologic regime, the lake shore aquifers of the proglacial lakes
814 are experiencing frozen-unfrozen transition seasonally, and the dominant recharge of
815 glacial melting could be fluctuated significantly due to air temperature variation.
816 Therefore, future groundwater and hydrological studies can be extended to longtime

826 sampling and monitoring of stable isotopes and ^{222}Rn in different water endmembers
827 to reveal the seasonally hydrological and hydrogeological dynamics and their impacts
828 on local biogeochemical cycles and ecological systems. Special concerns would be
829 placed on how surface/groundwater interactions and the associated biogeochemical
830 processes in response to the seasonal frozen ground variations and glacier/snowpack
831 melting intensity.

Deleted: -

832

833 **5. Conclusion**

Deleted:

834 A ^{222}Rn continuous monitoring is conducted at Ximen Co Lake, a proglacial lake
835 located at the east QTP. A dynamic ^{222}Rn mass balance model constrained by radium
836 mass balance and water level fluctuation is used to quantify temporal distribution of
837 LGD of the lake. The obtained LGD over the monitoring time ranges from -23.7
838 mm d^{-1} to 80.9 mm d^{-1} , with an average of $10.3 \pm 8.2 \text{ mm d}^{-1}$. Thereafter, a three
839 endmember model consisting of the budgets of water, stable isotopes and Cl^- is used
840 to depict the hydrologic partitioning of the lake. Riverine inflow, lake water outflow
841 via surface runoff, and surface evaporation are estimated to be 135.6 mm d^{-1} , 141.5
842 mm d^{-1} and 5.2 mm d^{-1} , respectively. LGD derived nutrient loading is estimated to be
843 $785.4 \mu\text{mol m}^{-2} \text{ d}^{-1}$ and $3.2 \mu\text{mol m}^{-2} \text{ d}^{-1}$ for DIN and DIP, respectively. This study also
844 implicates that LGD constitutes relatively small portion of the proglacial hydrologic

Deleted: Upon depicting nutrient budget within the lake, the primary productivity is estimated to be $0.41 \text{ mol C m}^{-2} \text{ d}^{-1}$.

850 partitioning, however, delivers nearly a half of the nutrient loadings to the proglacial
851 lake.

852 This study presents the first attempt to quantify LGD and the associated nutrient
853 loadings to the proglacial lake of QTP. To our knowledge, there is almost no study on
854 the groundwater-lake water interaction in the high altitude proglacial lakes in QTP.

855 This study demonstrates that ^{222}Rn based approach can be used to investigate the
856 groundwater dynamics in the high altitude proglacial lakes. The method is

857 instructional to similar studies in other proglacial lakes in the QTP and elsewhere. [For](#)

858 [a comprehensive understanding the hydrological and biogeochemical dynamics in the](#)

859 [QTP, interdisciplinary and multi-approach integrated studies are in great need. Of](#)

860 [particular importance are the lake hydrology and groundwater surface water](#)

861 [interaction studies based on multiple approaches such as remote sensing products,](#)

862 [long term and high resolution observation of climatological parameters and isotopic](#)

863 [data](#).

864

865 **Acknowledgements**

866 This study was supported by grants from the National Natural Science Foundation of

867 China (NSFC, No.41572208) and (NSFC, 91747204), and the Research Grants

868 Council of Hong Kong Special Administrative Region, China (HKU17304815), [and](#)

Deleted: international,

Deleted: ,

Deleted: ,

Deleted: based constraining and
numerical modeling

Deleted: .

875 | [the seed fund program granted by HKU-ZIRI](#). The authors thank Mr. Buming Jiang
876 | for his kind help in the field works during the campaign and Ergang Lian for his help
877 | in stable isotope analysis. The authors thank Jessie Lai for her help in FIA analysis in
878 | School of Biological Sciences, HKU. Supporting data are included as in the files of
879 | supplementary information 2 and 3; Climatological data are purchased through
880 | <http://www.weatherdt.com/shop.html>; any additional data may be obtained from L.X.
881 | (email: xinluo@hku.hk);

882 | **References**

883 | Åberg, J., Jansson, M., and Jonsson, A.: Importance of water temperature and
884 | thermal stratification dynamics for temporal variation of surface water CO₂ in a
885 | boreal lake, *Journal of Geophysical Research: Biogeosciences* (2005–2012), 115,
886 | 10.1029/2009JG001085, 2010.

887 | Andermann, C., Longuevergne, L., Bonnet, S., Crave, A., Davy, P., and Gloaguen, R.:
888 | Impact of transient groundwater storage on the discharge of Himalayan rivers, *Nat*
889 | *Geosci*, 5, 127-132, Doi 10.1038/Ngeo1356, 2012.

890 | Anderson, L., Birks, J., Rover, J., and Guldager, N.: Controls on recent Alaskan lake
891 | changes identified from water isotopes and remote sensing, *Geophysical Research*
892 | *Letters*, 40, 3413-3418, 2013.

893 | Anderson, N. J., Saros, J. E., Bullard, J. E., Cahoon, S. M., McGowan, S., Bagshaw, E. A.,
894 | Barry, C. D., Bindler, R., Burpee, B. T., and Carrivick, J. L.: The Arctic in the Twenty-First
895 | Century: Changing Biogeochemical Linkages across a Paraglacial Landscape of
896 | Greenland, *BioScience*, 67, 118-133, 2017.

897 | Barry, R. G.: The status of research on glaciers and global glacier recession: a review,
898 | *Progress in Physical Geography*, 30, 285-306, 2006.

899 | Batlle-Aguilar, J., Harrington, G. A., Leblanc, M., Welch, C., and Cook, P. G.: Chemistry
900 | of groundwater discharge inferred from longitudinal river sampling, *Water Resour*
901 | *Res*, 50, 1550-1568, 10.1002/2013WR013591, 2014.

902 | Belanger, T. V., Mikutel, D. F., and Churchill, P. A.: Groundwater seepage nutrient
903 | loading in a Florida Lake, *Water Res*, 19, 773-781,
904 | [http://dx.doi.org/10.1016/0043-1354\(85\)90126-5](http://dx.doi.org/10.1016/0043-1354(85)90126-5), 1985.

Deleted: .

Formatted: Subscript

Formatted: Default Paragraph Font

906 Biskop, S., Maussion, F., Krause, P., and Fink, M.: Differences in the water-balance
907 components of four lakes in the southern-central Tibetan Plateau, *Hydrol Earth Syst*
908 *Sc*, 20, 209, 2016.

909 Blume, T., Krause, S., Meinikmann, K., and Lewandowski, J.: Upscaling lacustrine
910 groundwater discharge rates by fiber-optic distributed temperature sensing, *Water*
911 *Resour Res*, 49, 7929-7944, 10.1002/2012WR013215, 2013.

912 Böhner, J.: *Säkulare Klimaschwankungen und rezente Klimatrends Zentral-und*
913 *Hochasiens*, Goltze, 1996.

914 Böhner, J.: General climatic controls and topoclimatic variations in Central and High
915 Asia, *Boreas*, 35, 279-295, 2006.

916 Bolch, T., Kulkarni, A., Kääh, A., Huggel, C., Paul, F., Cogley, J. G., Frey, H., Kargel, J. S.,
917 Fujita, K., Scheel, M., Bajracharya, S., and Stoffel, M.: The State and Fate of
918 Himalayan Glaciers, *Science*, 336, 310-314, 2012.

919 Brown, L. E., Hannah, D. M., Milner, A. M., Soulsby, C., Hodson, A. J., and Brewer, M.
920 J.: Water source dynamics in a glacierized alpine river basin (Taillon-Gabiétous,
921 French Pyrénées), *Water Resour Res*, 42, 2006.

922 Burnett, W. C., Peterson, R. N., Santos, I. R., and Hicks, R. W.: Use of automated radon
923 measurements for rapid assessment of groundwater flow into Florida streams,
924 *Journal of Hydrology*, 380, 298-304, 2010.

925 Callegary, J. B., Kikuchi, C. P., Koch, J. C., Lilly, M. R., and Leake, S. A.: Review:
926 Groundwater in Alaska (USA), *Hydrogeol J*, 21, 25-39, 10.1007/s10040-012-0940-5,
927 2013.

928 Cole, J., Nina, J., and Caraco, F.: Atmospheric exchange of carbon dioxide in a
929 low-wind oligotrophic lake measured by the addition of SF₆, *Limnol Oceanogr*, 43,
930 647-656, 1998.

931 Cook, P., Lamontagne, S., Berhane, D., and Clark, J.: Quantifying groundwater
932 discharge to Cockburn River, southeastern Australia, using dissolved gas tracers
933 222Rn and SF₆, *Water Resour Res*, 42, 2006.

934 Cook, P. G., Favreau, G., Dighton, J. C., and Tickell, S.: Determining natural
935 groundwater influx to a tropical river using radon, chlorofluorocarbons and ionic
936 environmental tracers, *Journal of Hydrology*, 277, 74-88,
937 [http://dx.doi.org/10.1016/S0022-1694\(03\)00087-8](http://dx.doi.org/10.1016/S0022-1694(03)00087-8), 2003.

938 Corbett, D. R., Burnett, W. C., Cable, P. H., and Clark, S. B.: Radon tracing of
939 groundwater input into Par Pond, Savannah River site, *Journal of Hydrology*, 203,
940 209-227, 1997.

941 Cui, X., Ren, J., Qin, X., Sun, W., Yu, G., Wang, Z., and Liu, W.: Chemical characteristics
942 and environmental records of a snow-pit at the Glacier No. 12 in the Laohugou Valley,
943 Qilian Mountains, *Journal of Earth Science*, 25, 379-385, 2014.

Deleted:-

Formatted: Subscript

Formatted: Default Paragraph Font

945 Dansgaard, W.: Stable isotopes in precipitation, *Tellus A*, 16, 1964.

946 Dimova, N., Paytan, A., Kessler, J. D., Sparrow, K., Garcia-Tigreros Kodovska, F., Lecher,
947 A. L., Murray, J., and Tulaczyk, S. M.: The current magnitude and mechanisms of
948 groundwater discharge in the Arctic: a case study from Alaska, *Environ Sci Technol*,
949 49, 12036-12043, 2015.

950 Dimova, N. T., and Burnett, W. C.: Evaluation of groundwater discharge into small
951 lakes based on the temporal distribution of radon-222, *Limnol. Oceanogr*, 56,
952 486-494, 2011.

953 Dimova, N. T., Burnett, W. C., Chanton, J. P., and Corbett, J. E.: Application of
954 radon-222 to investigate groundwater discharge into small shallow lakes, *Journal of*
955 *Hydrology*, 2013.

956 Downing, J. A., and McCauley, E.: The nitrogen: phosphorus relationship in lakes,
957 *Limnol Oceanogr*, 37, 936-945, 1992.

958 Dubnick, A., Wadham, J., Tranter, M., Sharp, M., Orwin, J., Barker, J., Bagshaw, E., and
959 Fitzsimons, S.: Trickle or treat: The dynamics of nutrient export from polar glaciers,
960 *Hydrol Process*, 31, 1776-1789, 10.1002/hyp.11149, 2017.

961 Einarsdottir, K., Wallin, M. B., and Sobek, S.: High terrestrial carbon load via
962 groundwater to a boreal lake dominated by surface water inflow, *Journal of*
963 *Geophysical Research: Biogeosciences*, [122 \(1\), 15-29](#), 10.1002/2016JG003495, 2017.

964 Farinotti, D., Longuevergne, L., Moholdt, G., Duethmann, D., Molg, T., Bolch, T.,
965 Vorogushyn, S., and Guntner, A.: Substantial glacier mass loss in the Tien Shan over
966 the past 50 years, *Nature Geosci*, 8, 716-722, 10.1038/ngeo2513
967 [http://www.nature.com/ngeo/journal/v8/n9/abs/ngeo2513.html#supplementary-inf](http://www.nature.com/ngeo/journal/v8/n9/abs/ngeo2513.html#supplementary-information)
968 [ormation](http://www.nature.com/ngeo/journal/v8/n9/abs/ngeo2513.html#supplementary-information), 2015.

969 Gat, J.: Stable isotopes of fresh and saline lakes, in: *Physics and chemistry of lakes*,
970 Springer, 139-165, 1995.

971 Gat, J.: Oxygen and hydrogen isotopes in the hydrologic cycle, *Annual Review of Earth*
972 *and Planetary Sciences*, 24, 225-262, 1996.

973 Genereux, D.: Quantifying uncertainty in tracer-based hydrograph separations, *Water*
974 *Resour Res*, 34, 915-919, 1998.

975 Gibson, J., Edwards, T., Bursey, G., and Prowse, T.: Estimating evaporation using stable
976 isotopes: quantitative results and sensitivity analysis for, *Nordic Hydrology*, 24, 79-94,
977 1993.

978 Gibson, J. J.: Short-term evaporation and water budget comparisons in shallow Arctic
979 lakes using non-steady isotope mass balance, *Journal of Hydrology*, 264, 242-261,
980 2002.

981 Gibson, J. J., and Edwards, T. W. D.: Regional water balance trends and
982 evaporation-transpiration partitioning from a stable isotope survey of lakes in

Deleted: n/a-n/a

Formatted: Default Paragraph Font

984 northern Canada, *Global Biogeochem Cy*, 16, 10-11-10-14, 10.1029/2001GB001839,
985 2002.

986 Gibson, J. J., Birks, S. J., and Yi, Y.: Stable isotope mass balance of lakes: a
987 contemporary perspective, *Quaternary Science Reviews*, 131, Part B, 316-328,
988 <http://dx.doi.org/10.1016/j.quascirev.2015.04.013>, 2016.

989 Gilfedder, B., Frei, S., Hofmann, H., and Cartwright, I.: Groundwater discharge to
990 wetlands driven by storm and flood events: Quantification using continuous
991 Radon-222 and electrical conductivity measurements and dynamic mass-balance
992 modelling, *Geochim Cosmochim Ac*, 165, 161-177, 2015.

993 Gonfiantini, R.: Environmental isotopes in lake studies, *Handbook of environmental*
994 *isotope geochemistry*, 2, 113-168, 1986.

995 Good, S. P., Noone, D., and Bowen, G.: Hydrologic connectivity constrains partitioning
996 of global terrestrial water fluxes, *Science*, 349, 175-177, 10.1126/science.aaa5931,
997 2015.

998 Hagerthey, S. E., and Kerfoot, W. C.: Groundwater flow influences the biomass and
999 nutrient ratios of epibenthic algae in a north temperate seepage lake, *Limnol*
1000 *Oceanogr*, 43, 1227-1242, 1998.

1001 Harris, C., Arenson, L. U., Christiansen, H. H., Etzelmüller, B., Frauenfelder, R., Gruber,
1002 S., Haeberli, W., Hauck, C., Hölzle, M., and Humlum, O.: Permafrost and climate in
1003 Europe: Monitoring and modelling thermal, geomorphological and geotechnical
1004 responses, *Earth-Science Reviews*, 92, 117-171, 2009.

1005 Hasler, C. T., Midway, S. R., Jeffrey, J. D., Tix, J. A., Sullivan, C., and Suski, C. D.:
1006 Exposure to elevated pCO₂ alters post-treatment diel movement patterns of
1007 largemouth bass over short time scales, *Freshwater Biology*, 61, 1590-1600,
1008 10.1111/fwb.12805, 2016.

1009 Hawkings, J., Wadham, J., Tranter, M., Telling, J., Bagshaw, E., Beaton, A., Simmons, S.
1010 L., Chandler, D., Tedstone, A., and Nienow, P.: The Greenland Ice Sheet as a hot spot
1011 of phosphorus weathering and export in the Arctic, *Global Biogeochem Cy*, [30 \(2\)](#),
1012 [191-210](#), 2016.

1013 Heckmann, T., McColl, S., and Morche, D.: Retreating ice: research in pro-glacial areas
1014 matters, *Earth Surface Processes and Landforms*, 41, 271-276, 10.1002/esp.3858,
1015 2016.

1016 Hodson, A., Mumford, P., Kohler, J., and Wynn, P. M.: The High Arctic glacial
1017 ecosystem: new insights from nutrient budgets, *Biogeochemistry*, 72, 233-256, 2005.

1018 Hodson, A.: Phosphorus in glacial meltwaters, *Glacier Science and Environmental*
1019 *Change*, 81-82, 2007.

1020 Hood, J. L., Roy, J. W., and Hayashi, M.: Importance of groundwater in the water
1021 balance of an alpine headwater lake, *Geophysical Research Letters*, 33,

Formatted: Default Paragraph Font

Deleted: Heckmann, T., McColl, S., and Morche, D.: Retreating ice: research in pro-glacial areas matters, *Earth Surface Processes and Landforms*, 2015. .

1026 10.1029/2006GL026611, 2006.

1027 Hren, M. T., Bookhagen, B., Blisniuk, P. M., Booth, A. L., and Chamberlain, C. P.: $\delta^{18}\text{O}$
1028 and δD of streamwaters across the Himalaya and Tibetan Plateau: Implications for
1029 moisture sources and paleoelevation reconstructions, *Earth Planet Sc Lett*, 288,
1030 20-32, 2009.

1031 Hudson, J. J., Taylor, W. D., and Schindler, D. W.: Phosphate concentrations in lakes,
1032 *Nature*, 406, 54-56, 2000.

1033 Johannes, R. E.: The Ecological Significance of the Submarine Discharge of
1034 Groundwater, *Mar Ecol-Prog Ser*, 3, 365-373, 1980.

1035 Kim, G., Burnett, W. C., Dulaiova, H., Swarzenski, P. W., and Moore, W. S.:
1036 Measurement of Ra-224 and Ra-226 activities in natural waters using a radon-in-air
1037 monitor, *Environ Sci Technol*, 35, 4680-4683, 2001.

1038 Klaus, J., and McDonnell, J.: Hydrograph separation using stable isotopes: Review and
1039 evaluation, *Journal of Hydrology*, 505, 47-64, 2013.

1040 Kluge, T., Ilmberger, J., Rohden, C. v., and Aeschbach-Hertig, W.: Tracing and
1041 quantifying groundwater inflow into lakes using a simple method for radon-222
1042 analysis, *Hydrol Earth Syst Sc*, 11, 1621-1631, 2007.

1043 Kluge, T., von Rohden, C., Sonntag, P., Lorenz, S., Wieser, M., Aeschbach-Hertig, W.,
1044 and Ilmberger, J.: Localising and quantifying groundwater inflow into lakes using
1045 high-precision ^{222}Rn profiles, *Journal of Hydrology*, 450, 70-81, 2012.

1046 Kraemer, T. F.: Radium isotopes in Cayuga Lake, New York: Indicators of inflow and
1047 mixing processes, *Limnol Oceanogr*, 50, 158-168, 2005.

1048 LaBaugh, J. W., Rosenberry, D. O., and Winter, T. C.: Groundwater contribution to the
1049 water and chemical budgets of Williams Lake, Minnesota, 1980-1991, *Can J Fish*
1050 *Aquat Sci*, 52, 754-767, 1995.

1051 LaBaugh, J. W., Winter, T. C., Rosenberry, D. O., Schuster, P. F., Reddy, M. M., and
1052 Aiken, G. R.: Hydrological and chemical estimates of the water balance of a closed-
1053 basin lake in north central Minnesota, *Water Resour Res*, 33, 2799-2812, 1997.

1054 Langston, G., Hayashi, M., and Roy, J. W.: Quantifying groundwater-surface water
1055 interactions in a proglacial moraine using heat and solute tracers, *Water Resour Res*,
1056 49, 5411-5426, 10.1002/wrcr.20372, 2013.

1057 Lazar, B., Weinstein, Y., Paytan, A., Magal, E., Bruce, D., and Kolodny, Y.: Ra and Th
1058 adsorption coefficients in lakes—Lake Kinneret (Sea of Galilee)“natural experiment”,
1059 *Geochim Cosmochim Ac*, 72, 3446-3459, 2008.

1060 Lazhu, Yang, K., Wang, J., Lei, Y., Chen, Y., Zhu, L., Ding, B., and Qin, J.: Quantifying
1061 evaporation and its decadal change for Lake Nam Co, central Tibetan Plateau, *Journal*
1062 *of Geophysical Research (Atmospheres)*, 121, 7578-7591, 2016.

1063 Lecher, A. L., Kessler, J., Sparrow, K., Garcia-Tigeros Kodovska, F., Dimova, N., Murray,

Deleted: <sup>

Formatted: Superscript

Deleted: </sup>

Deleted: <sup>

Formatted: Superscript

Deleted: </sup>

1068 J., Tulaczyk, S., and Paytan, A.: Methane transport through submarine groundwater
1069 discharge to the North Pacific and Arctic Ocean at two Alaskan sites, *Limnol Oceanogr*,
1070 [61 \(S1\), S344-355](#), 2015.

1071 Lee, C. M., Jiao, J. J., Luo, X., and Moore, W. S.: Estimation of submarine groundwater
1072 discharge and associated nutrient fluxes in Tolo Harbour, Hong Kong, *Sci Total Environ*,
1073 433, 427-433, [10.1016/j.scitotenv.2012.06.073](#), 2012.

1074 Lee, D. R.: A device for measuring seepage flux in lakes and estuaries, *Limnol*
1075 *Oceanogr*, 22, 140-147, 1977.

1076 Lee, D. R., Cherry, J. A., and Pickens, J. F.: Groundwater transport of a salt tracer
1077 through a sandy lakebed, *Limnol Oceanogr*, 25, 45-61, 1980.

1078 Lehmkühl, F.: Extent and spatial distribution of Pleistocene glaciations in eastern
1079 Tibet, *Quatern Int*, 45-46, 123-134,
1080 [http://dx.doi.org/10.1016/S1040-6182\(97\)00010-4](http://dx.doi.org/10.1016/S1040-6182(97)00010-4), 1998.

1081 Lei, Y., Yao, T., Yang, K., Sheng, Y., Kleinherenbrink, M., Yi, S., Bird, B. W., Zhang, X.,
1082 Zhu, L., and Zhang, G.: Lake seasonality across the Tibetan Plateau and their varying
1083 relationship with regional mass changes and local hydrology, *Geophysical Research*
1084 *Letters*, 44, 892-900, 2017.

1085 Lemieux, J. M., Sudicky, E. A., Peltier, W. R., and Tarasov, L.: Dynamics of groundwater
1086 recharge and seepage over the Canadian landscape during the Wisconsinian
1087 glaciation, *Journal of Geophysical Research: Earth Surface (2003–2012)*, 113,
1088 [10.1029/2007JF000838](#), 2008a.

1089 Lemieux, J. M., Sudicky, E. A., Peltier, W. R., and Tarasov, L.: Simulating the impact of
1090 glaciations on continental groundwater flow systems: 1. Relevant processes and
1091 model formulation, *Journal of Geophysical Research: Earth Surface*, 113, n/a-n/a,
1092 [10.1029/2007JF000928](#), 2008b.

1093 Lemieux, J. M., Sudicky, E. A., Peltier, W. R., and Tarasov, L.: Simulating the impact of
1094 glaciations on continental groundwater flow systems: 2. Model application to the
1095 Wisconsinian glaciation over the Canadian landscape, *Journal of Geophysical*
1096 *Research: Earth Surface (2003–2012)*, 113, [10.1029/2007JF000929](#), 2008c.

1097 Lerman, A., Imboden, D., and Gat, J.: *Physics and chemistry of lakes*, New York, 1995.

1098 Levy, A., Robinson, Z., Krause, S., Waller, R., and Weatherill, J.: Long-term variability
1099 of proglacial groundwater-fed hydrological systems in an area of glacier retreat,
1100 Skeiðarársandur, Iceland, *Earth Surface Processes and Landforms*, 40, 981-994,
1101 [10.1002/esp.3696](#), 2015.

1102 Lewandowski, J., Meinikmann, K., Ruhtz, T., Pöschke, F., and Kirillin, G.: Localization of
1103 lacustrine groundwater discharge (LGD) by airborne measurement of thermal
1104 infrared radiation, *Remote Sens Environ*, 138, 119-125,
1105 <http://dx.doi.org/10.1016/j.rse.2013.07.005>, 2013.

Formatted: Default Paragraph Font

Formatted: Default Paragraph Font

1106 Lewandowski, J., Meinikmann, K., Nützmann, G., and Rosenberry, D. O.: Groundwater
1107 – the disregarded component in lake water and nutrient budgets. Part 2: effects of
1108 groundwater on nutrients, *Hydrol Process*, 29, 2922-2955, 10.1002/hyp.10384, 2015.
1109 Li, Y. H., and Gregory, S.: Diffusion of Ions in Sea-Water and in Deep-Sea Sediments,
1110 *Geochim Cosmochim Ac*, 38, 703-714, 1974.
1111 Liu, C., Liu, J., Wang, X. S., and Zheng, C.: Analysis of groundwater–lake interaction by
1112 distributed temperature sensing in Badain Jaran Desert, Northwest China, *Hydrol*
1113 *Process*, [30 \(9\), 1330-1341](#), 2015.
1114 Liu, Y., Yao, T., Jiao, N., Tian, L., Hu, A., Yu, W., and Li, S.: Microbial diversity in the
1115 snow, a moraine lake and a stream in Himalayan glacier, *Extremophiles*, 15, 411-421,
1116 2011.
1117 Luo, X., Jiao, J. J., Moore, W., and Lee, C. M.: Submarine groundwater discharge
1118 estimation in an urbanized embayment in Hong Kong via short-lived radium isotopes
1119 and its implication of nutrient loadings and primary production, *Mar Pollut Bull*, 82,
1120 144-154, 2014.
1121 Luo, X., and Jiao, J. J.: Submarine groundwater discharge and nutrient loadings in Tolo
1122 Harbor, Hong Kong using multiple geotracer-based models, and their implications of
1123 red tide outbreaks, *Water Res*, 102, 11-31,
1124 <http://dx.doi.org/10.1016/j.watres.2016.06.017>, 2016.
1125 Luo, X., Jiao, J. J., Wang, X.-s., and Liu, K.: Temporal ²²²Rn distributions to reveal
1126 groundwater discharge into desert lakes: implication of water balance in the Badain
1127 Jaran Desert, China, *Journal of Hydrology*, 534, 87-103, 2016.
1128 Luo, X., Jiao, J. J., Wang, X.-s., Liu, K., Lian, E., and Yang, S.: Groundwater discharge
1129 and hydrologic partition of the lakes in desert environment: Insights from stable
1130 ¹⁸O/²H and radium isotopes, *Journal of Hydrology*, 546, 189-203, 2017.
1131 Luo, X., Jiao, J. J., Liu, Y., Zhang, X., Liang, W., and Tang, D.: Evaluation of Water
1132 Residence Time, Submarine Groundwater Discharge, and Maximum New Production
1133 Supported by Groundwater Borne Nutrients in a Coastal Upwelling Shelf System,
1134 *Journal of Geophysical Research: Oceans*, 123, 631-655, 2018.
1135 Ma, N., Zhang, Y., Szilagyi, J., Guo, Y., Zhai, J., and Gao, H.: Evaluating the
1136 complementary relationship of evapotranspiration in the alpine steppe of the
1137 Tibetan Plateau, *Water Resour Res*, 51, 1069-1083, 10.1002/2014WR015493, 2015.
1138 MacIntyre, S., Wannikhof, R., Chanton, J. P., Matson, P. A., and Hariss, R. C.: Biogenic
1139 Trace Gases: Measuring Emissions from Soil and Water, 52 pp., 1995.
1140 Magnusson, J., Kobierska, F., Huxol, S., Hayashi, M., Jonas, T., and Kirchner, J. W.: Melt
1141 water driven stream and groundwater stage fluctuations on a glacier forefield
1142 (Dammagletscher, Switzerland), *Hydrol Process*, 28, 823-836, 2014.
1143 Mitamura, O., Seike, Y., Kondo, K., Goto, N., Anbutsu, K., Akatsuka, T., Kihira, M.,

Formatted: Default Paragraph Font

Formatted: Superscript

Deleted:

Formatted: Superscript

Deleted:

Formatted: Superscript

Deleted:

1147 Tsering, T. Q., and Nishimura, M.: First investigation of ultraoligotrophic alpine Lake
1148 Puma Yumco in the pre-Himalayas, China, *Limnology*, 4, 167-175, 2003.

1149 Moore, W. S.: Sampling radium-228 in the deep ocean, *Deep Sea Res.*, 23, 647-651,
1150 1976.

1151 Nakayama, T., and Watanabe, M.: Missing role of groundwater in water and nutrient
1152 cycles in the shallow eutrophic Lake Kasumigaura, Japan, *Hydrol Process*, 22,
1153 1150-1172, 2008.

1154 Paytan, A., Lecher, A. L., Dimova, N., Sparrow, K. J., Kodovska, F. G.-T., Murray, J.,
1155 Tulaczyk, S., and Kessler, J. D.: Methane transport from the active layer to lakes in the
1156 Arctic using Toolik Lake, Alaska, as a case study, *Proceedings of the National Academy
1157 of Sciences*, 112, 3636-3640, 2015.

1158 Qiu, J.: China: the third pole, *Nature News*, 454, 393-396, 2008.

1159 Quigley, M. A., and Robbins, J. A.: Phosphorus release processes in nearshore
1160 southern Lake Michigan, *Can J Fish Aquat Sci*, 43, 1201-1207, 1986.

1161 Ren, W., Yao, T., Yang, X., and Joswiak, D. R.: Implications of variations in $\delta^{18}\text{O}$ and δD
1162 in precipitation at Madoi in the eastern Tibetan Plateau, *Quatern Int*, 313-314, 56-61,
1163 <https://doi.org/10.1016/j.quaint.2013.05.026>, 2013.

1164 Ren, W., Yao, T., Xie, S., and He, Y.: Controls on the stable isotopes in precipitation
1165 and surface waters across the southeastern Tibetan Plateau, *Journal of Hydrology*,
1166 545, 276-287, <http://dx.doi.org/10.1016/j.jhydrol.2016.12.034>, 2017.

1167 Rosenberry, D. O., Lewandowski, J., Meinikmann, K., and Nützmann, G.:
1168 Groundwater-the disregarded component in lake water and nutrient budgets. Part 1:
1169 effects of groundwater on hydrology, *Hydrol Process*, 29, 2895-2921, 2015.

1170 Roy, J. W., and Hayashi, M.: Groundwater exchange with two small alpine lakes in the
1171 Canadian Rockies, *Hydrol Process*, 22, 2838-2846, 2008.

1172 Schafran, G. C., and Driscoll, C. T.: Flow path - composition relationships for
1173 groundwater entering an acidic lake, *Water Resour Res*, 29, 145-154, 1993.

1174 Scheidegger, J. M., and Bense, V. F.: Impacts of glacially recharged groundwater flow
1175 systems on talik evolution, *Journal of Geophysical Research: Earth Surface*, 119,
1176 758-778, 10.1002/2013JF002894, 2014.

1177 Schlutz, F., and Lehmkuhl, F.: Holocene climatic change and the nomadic
1178 Anthropocene in Eastern Tibet: palynological and geomorphological results from the
1179 Nianbaoyeze Mountains, *Quaternary Science Reviews*, 28, 1449-1471, 2009.

1180 Schmidt, A., Gibson, J. J., Santos, I. R., Schubert, M., Tattrie, K., and Weiss, H.: The
1181 contribution of groundwater discharge to the overall water budget of two typical
1182 Boreal lakes in Alberta/Canada estimated from a radon mass balance, *Hydrol Earth
1183 Syst Sc*, 14, 79-89, 2010.

1184 Sebok, E., Duque, C., Kazmierczak, J., Engesgaard, P., Nilsson, B., Karan, S., and

Formatted: Superscript

Formatted: Default Paragraph Font

Formatted: Default Paragraph Font

Formatted: Font: (Default) Times New Roman

1185 Frandsen, M.: High-resolution distributed temperature sensing to detect seasonal
1186 groundwater discharge into Lake Væng, Denmark, *Water Resour Res*, 49, 5355-5368,
1187 2013.

1188 Shaw, R. D., and Prepas, E. E.: Groundwater-lake interactions: I. Accuracy of seepage
1189 meter estimates of lake seepage, *Journal of Hydrology*, 119, 105-120,
1190 [http://dx.doi.org/10.1016/0022-1694\(90\)90037-X](http://dx.doi.org/10.1016/0022-1694(90)90037-X), 1990.

1191 Slaymaker, O.: Criteria to distinguish between periglacial, proglacial and paraglacial
1192 environments, *Quaestiones Geographicae*, 30, 85-94, 2011.

1193 Slomp, C. P., and Van Cappellen, P.: Nutrient inputs to the coastal ocean through
1194 submarine groundwater discharge: controls and potential impact, *Journal of*
1195 *Hydrology*, 295, 64-86, Doi 10.1016/J.jhyfrol.2004.02.018, 2004.

1196 Smerdon, B., Mendoza, C., and Devito, K.: Simulations of fully coupled lake-
1197 groundwater exchange in a subhumid climate with an integrated hydrologic model,
1198 *Water Resour Res*, 43, 2007.

1199 Stets, E. G., Winter, T. C., Rosenberry, D. O., and Striegl, R. G.: Quantification of
1200 surface water and groundwater flows to open- and closed-basin lakes in a
1201 headwaters watershed using a descriptive oxygen stable isotope model, *Water*
1202 *Resour Res*, 46, 10.1029/2009WR007793, 2010.

1203 Tockner, K., Malard, F., Uehlinger, U., and Ward, J.: Nutrients and organic matter in a
1204 glacial river-floodplain system (Val Roseg, Switzerland), *Limnol Oceanogr*, 47, 266-277,
1205 2002.

1206 Valiela, I., Teal, J. M., Volkmann, S., Shafer, D., and Carpenter, E. J.: Nutrient and
1207 Particulate Fluxes in a Salt-Marsh Ecosystem - Tidal Exchanges and Inputs by
1208 Precipitation and Groundwater, *Limnol Oceanogr*, 23, 798-812, 1978.

1209 Wang, C., Dong, Z., Qin, X., Zhang, J., Du, W., and Wu, J.: Glacier meltwater runoff
1210 process analysis using δD and $\delta^{18}O$ isotope and chemistry at the remote Laohugou
1211 glacier basin in western Qilian Mountains, China, *Journal of Geographical Sciences*,
1212 26, 722-734, 2016a.

1213 Wang, J., Zhu, L., Wang, Y., Ju, J., Xie, M., and Daut, G.: Comparisons between the
1214 chemical compositions of lake water, inflowing river water, and lake sediment in Nam
1215 Co, central Tibetan Plateau, China and their controlling mechanisms, *Journal of Great*
1216 *Lakes Research*, 36, 587-595, 2010.

1217 Wang, R., Liu, Z., Jiang, L., Yao, Z., Wang, J., and Ju, J.: Comparison of surface water
1218 chemistry and weathering effects of two lake basins in the Changtang Nature Reserve,
1219 China, *Journal of Environmental Sciences*, 41, 183-194,
1220 <http://dx.doi.org/10.1016/j.jes.2015.03.016>, 2016b.

1221 Wang, S.: Frozen ground and environment in the Zoige Plateau and its surrounding
1222 mountains (In Chinese with English abstract), *Journal of Glaciology and Geocryology*,

Formatted: Default Paragraph Font

Formatted: Default Paragraph Font

1223 19, 39-46, 1997.

1224 Warner, N. R., Christie, C. A., Jackson, R. B., and Vengosh, A.: Impacts of shale gas
1225 wastewater disposal on water quality in western Pennsylvania, *Environ Sci Technol*,
1226 47, 11849-11857, 2013.

1227 Weynell, M., Wiechert, U., and Zhang, C.: Chemical and isotopic (O, H, C) composition
1228 of surface waters in the catchment of Lake Donggi Cona (NW China) and implications
1229 for paleoenvironmental reconstructions, *Chemical Geology*, 435, 92-107,
1230 <http://dx.doi.org/10.1016/j.chemgeo.2016.04.012>, 2016.

1231 White, D., Lapworth, D. J., Stuart, M. E., and Williams, P. J.: Hydrochemical profiles in
1232 urban groundwater systems: New insights into contaminant sources and pathways in
1233 the subsurface from legacy and emerging contaminants, *Sci Total Environ*, 562,
1234 962-973, <http://dx.doi.org/10.1016/j.scitotenv.2016.04.054>, 2016.

1235 Wilson, J., and Rocha, C.: A combined remote sensing and multi-tracer approach for
1236 localising and assessing groundwater-lake interactions, *International Journal of*
1237 *Applied Earth Observation and Geoinformation*, 44, 195-204, 2016.

1238 Winter, T. C.: Relation of streams, lakes, and wetlands to groundwater flow systems,
1239 *Hydrogeol J*, 7, 28-45, 1999.

1240 Wischniewski, J., Herzsich, U., Rühland, K. M., Bräuning, A., Mischke, S., Smol, J. P.,
1241 and Wang, L.: Recent ecological responses to climate variability and human impacts
1242 in the Nianbaoyeze Mountains (eastern Tibetan Plateau) inferred from pollen, diatom
1243 and tree-ring data, *Journal of paleolimnology*, 51, 287-302, 2014.

1244 Xin, W., Yongjian, D., Shiyin, L., Lianghong, J., Kunpeng, W., Zongli, J., and Wanqin, G.:
1245 Changes of glacial lakes and implications in Tian Shan, central Asia, based on remote
1246 sensing data from 1990 to 2010, *Environmental Research Letters*, 8, 044052, 2013.

1247 Yang, K., Wu, H., Qin, J., Lin, C., Tang, W., and Chen, Y.: Recent climate changes over
1248 the Tibetan Plateau and their impacts on energy and water cycle: A review, *Global*
1249 *and Planetary Change*, 112, 79-91, 2014.

1250 Yao, T., Thompson, L., Yang, W., Yu, W., Gao, Y., Guo, X., Yang, X., Duan, K., Zhao, H.,
1251 Xu, B., Pu, J., Lu, A., Xiang, Y., Kattel, D. B., and Joswiak, D.: Different glacier status
1252 with atmospheric circulations in Tibetan Plateau and surroundings, *Nature Clim.*
1253 *Change*, 2, 663-667,
1254 [http://www.nature.com/nclimate/journal/v2/n9/abs/nclimate1580.html#supplemen](http://www.nature.com/nclimate/journal/v2/n9/abs/nclimate1580.html#supplementary-information)
1255 [tary-information](http://www.nature.com/nclimate/journal/v2/n9/abs/nclimate1580.html#supplementary-information), 2012.

1256 Yao, T., Masson-Delmotte, V., Gao, J., Yu, W., Yang, X., Risi, C., Sturm, C., Werner, M.,
1257 Zhao, H., He, Y., Ren, W., Tian, L., Shi, C., and Hou, S.: A review of climatic controls on
1258 $\delta^{18}\text{O}$ in precipitation over the Tibetan Plateau: Observations and simulations,
1259 *Reviews of Geophysics*, 51, 525-548, 10.1002/rog.20023, 2013.

1260 Yao, Z., Wang, R., Liu, Z., Wu, S., and Jiang, L.: Spatial-temporal patterns of major ion

Formatted: Default Paragraph Font

Formatted: Default Paragraph Font

Formatted: Default Paragraph Font

1261 chemistry and its controlling factors in the Manasarovar Basin, Tibet, *Journal of*
1262 *Geographical Sciences*, 25, 687-700, 10.1007/s11442-015-1196-5, 2015.

1263 Yuan, H., Liu, E., Shen, J., Zhou, H., Geng, Q., and An, S.: Characteristics and origins of
1264 heavy metals in sediments from Ximen Co Lake during summer monsoon season, a
1265 deep lake on the eastern Tibetan Plateau, *J Geochem Explor*, 136, 76-83,
1266 <http://dx.doi.org/10.1016/j.gexplo.2013.10.008>, 2014.

1267 Zhang, B., Wu, Y., Zhu, L., Wang, J., Li, J., and Chen, D.: Estimation and trend
1268 detection of water storage at Nam Co Lake, central Tibetan Plateau, *Journal of*
1269 *Hydrology*, 405, 161-170, 2011.

1270 Zhang, C., and Mischke, S.: A Lateglacial and Holocene lake record from the
1271 Nianbaoyeze Mountains and inferences of lake, glacier and climate evolution on the
1272 eastern Tibetan Plateau, *Quaternary Science Reviews*, 28, 1970-1983, 2009.

1273 Zhang, G., Yao, T., Xie, H., Kang, S., and Lei, Y.: Increased mass over the Tibetan
1274 Plateau: from lakes or glaciers?, *Geophysical Research Letters*, 40, 2125-2130, 2013.

1275 Zhang, G., Yao, T., Piao, S., Bolch, T., Xie, H., Chen, D., Gao, Y., O'Reilly, C. M., Shum, C.,
1276 and Yang, K.: Extensive and drastically different alpine lake changes on Asia's high
1277 plateaus during the past four decades, *Geophysical Research Letters*, 44, 252-260,
1278 2017a.

1279 Zhang, G., Yao, T., Shum, C., Yi, S., Yang, K., Xie, H., Feng, W., Bolch, T., Wang, L., and
1280 Behrangi, A.: Lake volume and groundwater storage variations in Tibetan Plateau's
1281 endorheic basin, *Geophysical Research Letters*, 44, 5550-5560, 2017b.

1282 Zhang, Y., Liu, C., Tang, Y., and Yang, Y.: Trends in pan evaporation and reference and
1283 actual evapotranspiration across the Tibetan Plateau, *Journal of Geophysical*
1284 *Research: Atmospheres* (1984–2012), 112, 10.1029/2006JD008161, 2007.

1285 Zhou, S., Kang, S., Chen, F., and Joswiak, D. R.: Water balance observations reveal
1286 significant subsurface water seepage from Lake Nam Co, south-central Tibetan
1287 Plateau, *Journal of Hydrology*, 491, 89-99, 2013.

1288 Zlotnik, V. A., Olaguera, F., and Ong, J. B.: An approach to assessment of flow regimes
1289 of groundwater-dominated lakes in arid environments, *Journal of hydrology*, 371,
1290 22-30, 2009.

1291 Zlotnik, V. A., Robinson, N. I., and Simmons, C. T.: Salinity dynamics of discharge lakes
1292 in dune environments: Conceptual model, *Water Resour Res*, 46, 2010.

1293 Zongxing, L., Qi, F., Wei, L., Tingting, W., Xiaoyan, G., Zongjie, L., Yan, G., Yanhui, P.,
1294 Rui, G., and Bing, J.: The stable isotope evolution in Shiyi glacier system during the
1295 ablation period in the north of Tibetan Plateau, China, *Quatern Int*, 380, 262-271,
1296 2015.

1297

Formatted: Default Paragraph Font

1298 | **Figure captions**

1299

1300 **Figure 1** The geological and topographic map of the Yellow River Source Region,
1301 Nianbaoyeze glacial mountains (a), and the sampling settings of the Ximen Co Lake
1302 (b), with the bathymetry map of the lake (d). (c) Photograph of the Ximen Co Lake
1303 and the surrounding geomorphic settings looking northeast direction on 22 Aug 2015,
1304 showing the late-laying snowpack in the U-shaped valleys of the north part of
1305 Nianbaoyeze MT.

1306

1307 **Figure 2** The climatological parameters (wind speed, air temperature, and
1308 precipitation) in the Aug, 2015 recorded from Jiuzhi weather station.

1309

1310 **Figure 3** The temporal distributions of ^{222}Rn (a), water temperature (b), water level
1311 fluctuation recorded by the divers (c), and hourly wind speed and air temperature
1312 recorded in Jiuzhi weather station (d).

1313

1314 **Figure 4** The cross plots of Cl^- versus Na^+ (a), SO_4^{2-} versus Cl^- (b), Ca^{2+} versus Cl^-
1315 (c); The relations of ^2H versus ^{18}O (d), Cl^- versus ^2H (e), and Cl^- versus ^{18}O (f).

1316

1317 **Figure 5** Cross plots of ^{222}Rn versus DIN (a) and DIP (b).

1318

1319 **Figure 6** The conceptual model of ^{222}Rn transient model (a), and three endmember
1320 model (b).

1321

1322 **Figure 7** The results of the final LGD derived from ^{222}Rn transient model.

1323

1324 **Figure 8** The hydrologic partition of the proglacial lake of Ximen CO (a), and the
1325 budgets of DIN (b) and DIP (c).

1326

1327

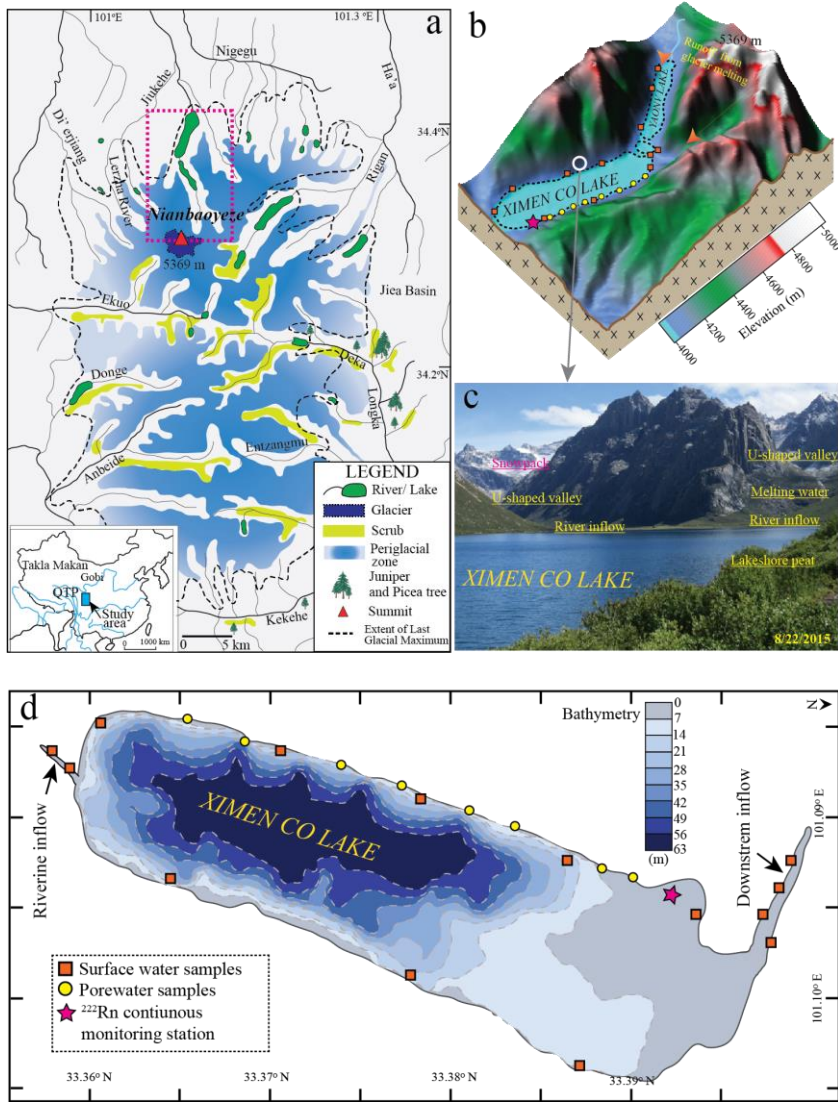
1328

1329

1330

Deleted: -

-



1334

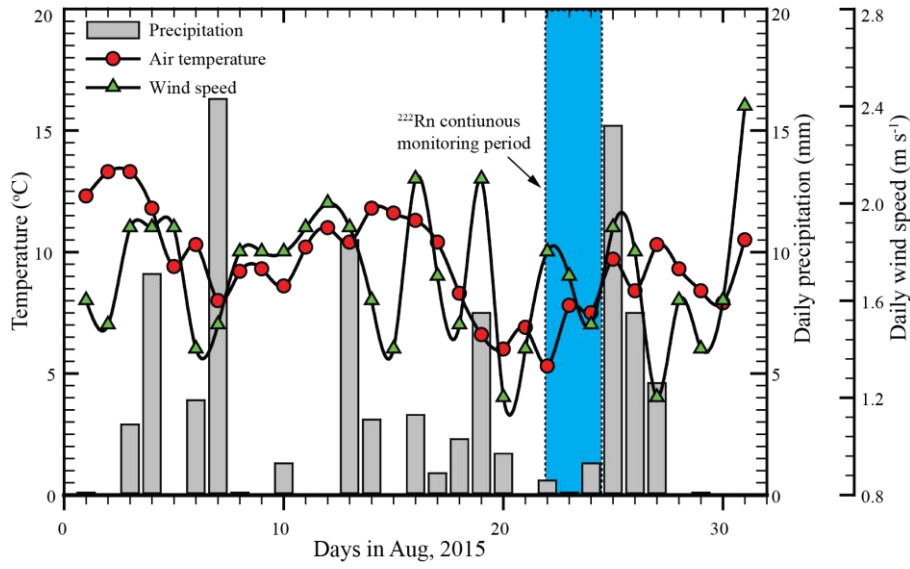
1335

1336

1337

1338

1339 Figure 2



1340

1341

1342

1343

1344

1345

1346

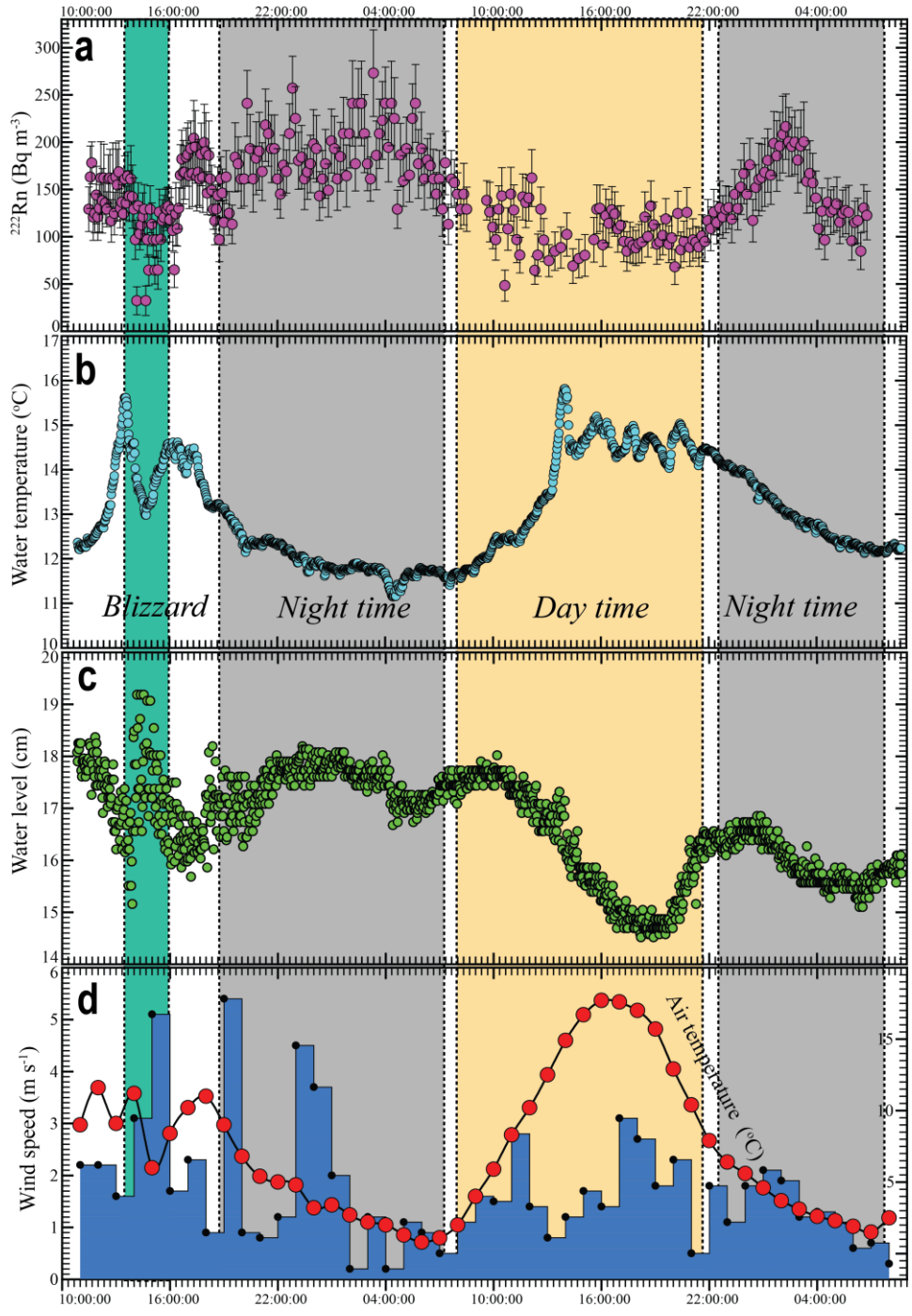
1347

1348

1349

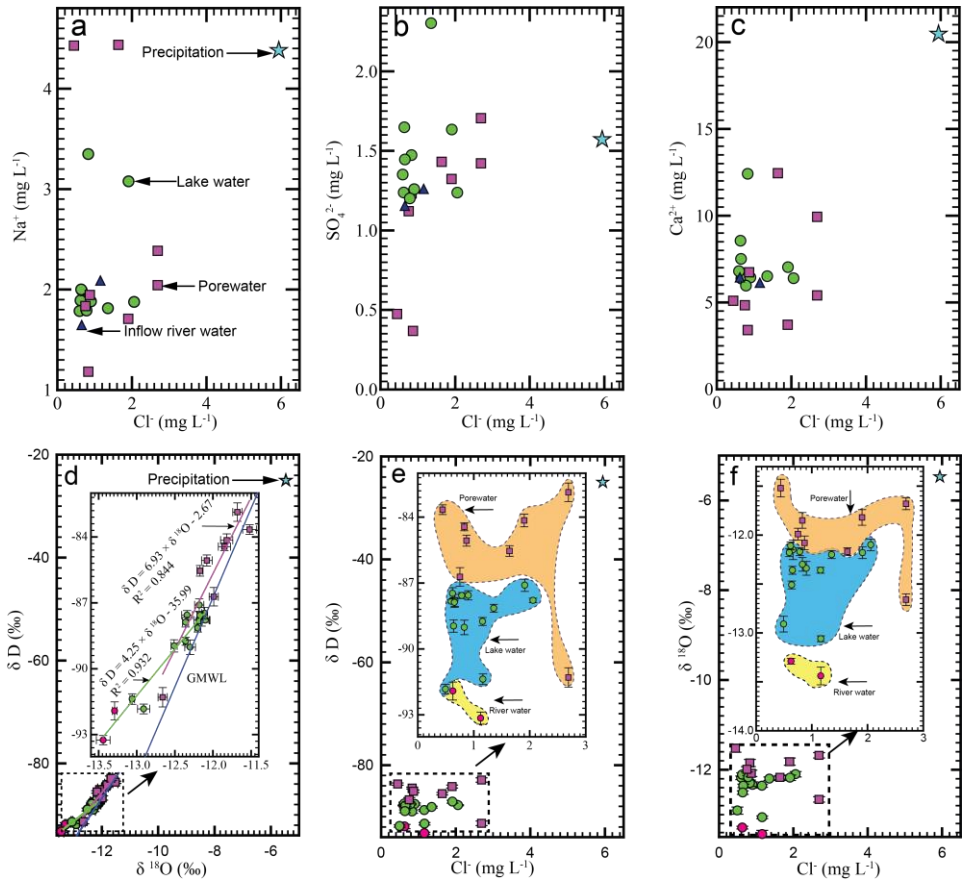
1350

1351



1355

Figure 4



1356

1357

1358

1359

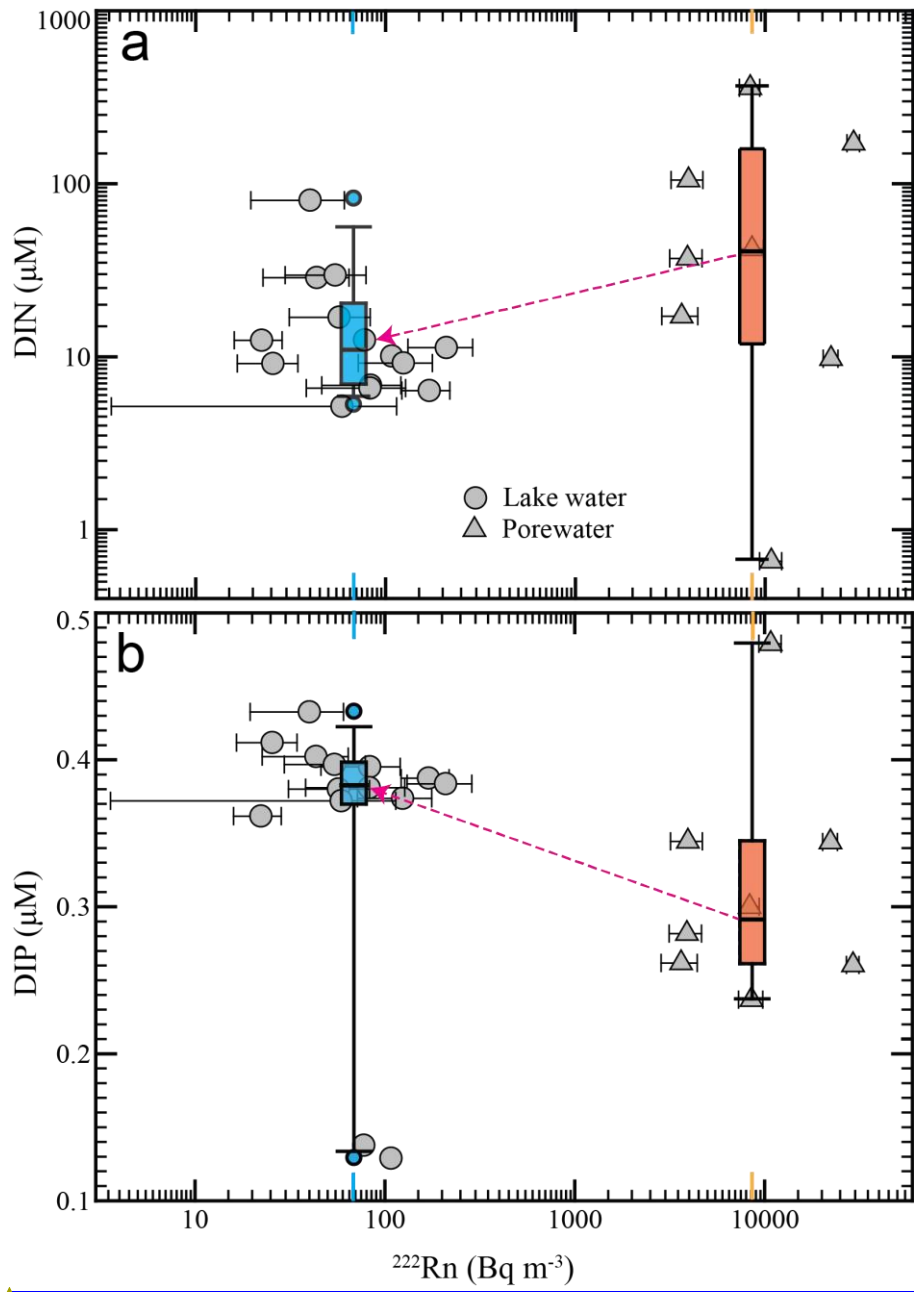
1360

1361

1362

1363

Figure 5

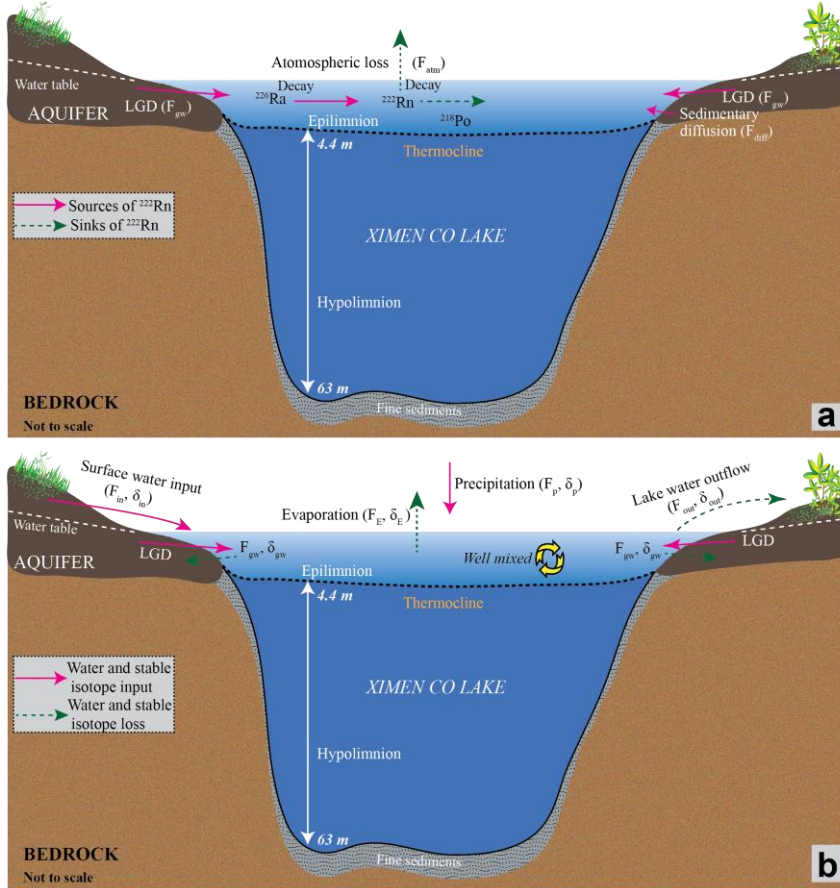


Formatted: Font: (Default) Times New Roman, (Asian) 宋体, 11 pt

Formatted: Indent: Left: 0 cm, Hanging: 1

1368

Figure 6



Deleted: .
.
.
.

1369

1370

1371

1372

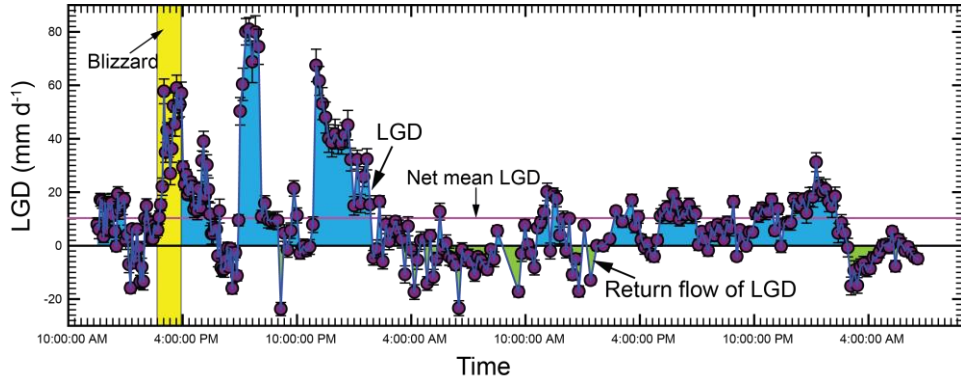
1373

1374

1375

1376

1381 Figure 7



1382

1383

1384

1385

1386

1387

1388

1389

1390

1391

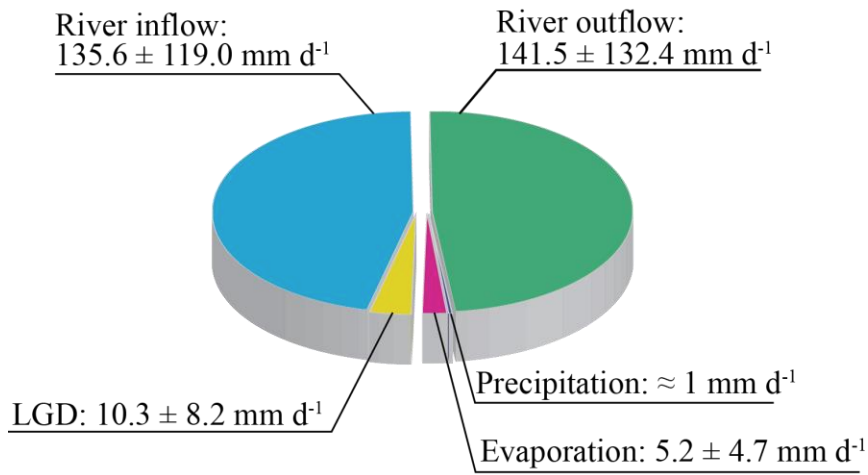
1392

1393

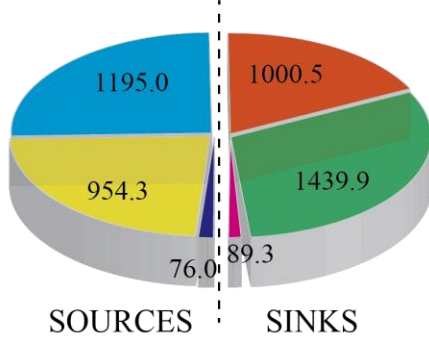
1394

1395

a Hydrologic partitioning



b DIN ($\mu\text{mol m}^{-2} \text{d}^{-1}$)



c DIP ($\mu\text{mol m}^{-2} \text{d}^{-1}$)

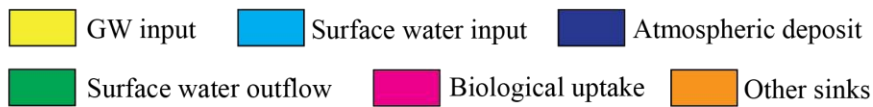
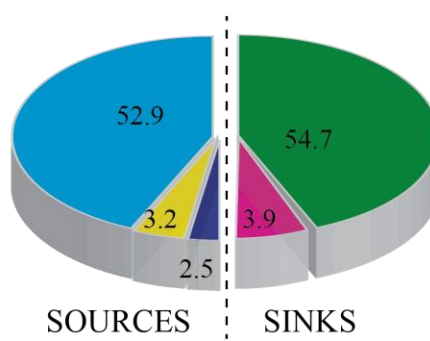


Table 1 Parameters used to establish the mass balance model of ^{222}Rn in Ximen Co Lake.

Parameters	Units or values	Estimated Uncertainty (%)	Evaluation
Wind speed (ω_{10})	0.2 - 5.4 m s ⁻¹	n.a	From Jiuzhi weather stations
Water-air temperature	11.2 - 15.6 °C	n.a	Recorded with probe in the chamber; sensitive to temperature results
Molecular diffusion of ^{222}Rn in water (D_m)	9.2×10^{-6} - 1.0×10^{-5} cm ² s ⁻¹	n.a	1.16×10^{-6} at 20 °C; adjustable for temperature
Molecular diffusion of ^{222}Rn in sediments (D_s)	2.2×10^{-6} - 2.5×10^{-5} cm ² s ⁻¹	n.a	Adjusted for temperature, sediment porosity
Dynamic viscosity (μ)	1.1×10^{-3} - 1.3×10^{-3} cm ² s ⁻¹	n.a	Calculated based on water temperature, density and salinity
Schmidt number (S_c)	1078.6 - 1371.6 [-]	n.a	Calculated as the ratio of ν to D_m
Water depth (H)	4.4 m	n.a	Epilimnion depth of Ximen Co Lake
Decay constant ^{222}Rn (λ_{222})	0.186 d ⁻¹	n.a	Constant
Groundwater endmember ^{222}Rn (C_{gw})	11200 ± 1200 Bq m ⁻³	8 sites dependant dependent for	Measured; final result for water flux inversely proportional to ^{222}Rn groundwater concentration
Lake water endmember ^{222}Rn (C_l)	21.6- 418.8 Bq m ⁻³	15-25%	Measured with RAD 7 AQUA
Ambient air ^{222}Rn (C_{air})	1.51 ± 0.97 Bq m⁻³	15-25 %	Measured with RAD 7 under open loop conditions
Atmospheric ^{222}Rn (C_a)	1.5 ± 1.0 Bq m ⁻³	20-25%	Measured or assumed value, model not sensitive to radon in air variation
$K_{\text{air/water}}$	0.29 - 0.33 [-]	n.a	Calculated based on temperature in the chamber and salinity in lake water
Porosity n	0.31	n.a	Assumed based on literatures
Tortuosity θ	2.05	n.a	Calculated based on porosity
Piston velocity (κ)	0.004 - 1.11 m d ⁻¹	20-25%	Calculated from Equation 3 in supplementary information
^{226}Ra concentration in lake waters (C_{226Ra})	0.01 Bq m ⁻³	≈10%	Measured with RAD7
Diffusive flux of ^{222}Rn (F_{diff})	0.68 - 213.5 Bq m ⁻² d ⁻¹	n.a	Calculated from Equation 9 in supplementary information
Atmospheric flux of ^{222}Rn (F_{atm})	0.7 - 213.5 Bq m ⁻² d ⁻¹	n.a	Calculated from Equation 1 in supplementary information
Groundwater flux of ^{222}Rn (F_{gw})	14.7 - 349.8 Bq m ⁻² d ⁻¹	n.a	Calculated from Equation 1
Inventory of ^{222}Rn (I)	Bq m ⁻²	n.a	Measured with RAD7 AQUA
Groundwater discharge (Q_{gw})	10.3 ± 8.2 (3.5-38.6) mm d ⁻¹	n.a	Calculated from Equation 1

Table 2 Input parameters for the three endmember model of Ximen Co Lake

Input parameter	Description	Values (using ^{18}O as a tracer)	Parametric sources
h	Relatively humidity	0.63	Measured by the humidity meter
T ($^{\circ}\text{C}$)	Water temperature	15.66	Monitored with divers
δ_{surface} (^{18}O) ‰	Surface water isotopic compositions	-12.45	Average value of surface inflow samples
δ_{gw} (^{18}O) ‰	Groundwater isotopic compositions	-11.97	Average value of porewater samples
δ_L (^{18}O) ‰	Lake water isotopic compositions	-12.54	Average value of Ximen Co Lake water samples
F_{gw} (mm/d)	LGD rates	14.18	Calculated based on ^{222}Rn mass balance model
ε^* (^{18}O) ‰	Effective equilibrium isotopic enrichment factor	10.12	Equations 13-14 in supplementary information
C_k (^{18}O) ‰	Kinetic constant for ^{18}O	14.2	Constants based on evaporating experiment
ε_k (^{18}O) ‰	Kinetic enrichment factor	5.2	From Equation 15 in supplementary information
ε (^{18}O) ‰	Total isotopic enrichment factor	15.33	The sum of ε^* and C_k
α^* (^{18}O) ‰	Effective isotopic equilibrium factor	1.01	$\alpha^*=1+\varepsilon^*$
δ_a (^{18}O) ‰	Isotopic composition of ambient air	-23.12	Estimated with δ_{in} and δ_a
δ_{in} (^{18}O) ‰	Isotopic composition of surface inflow water	-13.41	Average value of surface inflow water
δ_E (^{18}O) ‰	Isotopic compositions of evaporating vapor	-35.1	From Equation 12 in supplementary information
$[Cl]_{\text{in}}$ (mgL^{-1})	Chloride concentrations in surface inflow water	0.91	Filed data
$[Cl]_L$ (mgL^{-1})	Chloride concentrations in lake water	1.02	Filed data
$[Cl]_{\text{gw}}$ (mgL^{-1})	Chloride concentrations in groundwater	1.48	Filed data